FUNKTIONALANALYSIS UND GEOMATHEMATIK

M. J. Fengler, W. Freeden

A Nonlinear Galerkin Scheme Involving Vector and Tensor Spherical Harmonics for Solving the Incompressible Navier-Stokes Equation on the Sphere

FACHBEREICH MATHEMATIK

A NONLINEAR GALERKIN SCHEME INVOLVING VECTOR AND TENSOR SPHERICAL HARMONICS FOR SOLVING THE INCOMPRESSIBLE NAVIER-STOKES EQUATION ON THE SPHERE

M. J. FENGLER* AND W. FREEDEN*

Abstract. This work is concerned with a nonlinear Galerkin method for solving the incompressible Navier-Stokes equation on the sphere. It extends the work of [7, 17, 22] from one-dimensional or toroidal domains to the spherical geometry. In the first part, the method based on type 3 vector spherical harmonics is introduced and convergence is indicated. Further it is shown that the occurring coupling terms involving three vector spherical harmonics can be expressed algebraically in terms of Wigner-3j coefficients. To improve the numerical efficiency and economy we introduce an FFT based pseudo spectral algorithm for computing the Fourier coefficients of the nonlinear advection term. The resulting method scales with $O(N^3)$, if N denotes the maximal spherical harmonic degree. The latter is demonstrated in an extensive numerical example.

Key words. Incompressible Spherical Navier-Stokes Equation, Nonlinear Galerkin Scheme, Vector Spherical Harmonics, Pseudo Spectral Algorithm, Transform Method

AMS subject classifications. 76D05, 37L65, 33C55, 42A99, 85A20

1. Motivation. Spectral methods are well-known for solving different types of partial differential equations such as the Laplace, Helmholtz, heat or wave equations, but also for nonlinear equations such as the Burger, shallow water, or full Navier-Stokes equation, or even more complex coupled partial differential equations, e.g., known from dynamo theory, magneto-hydrodynamics, or meteorology (cf. [2, 3, 9, 12, 15, 19, 20, 21, 24]). Spectral methods are usually implemented in Galerkin schemes, which are applied to, for example, complex flows but in simple geometries, e.g., a two-dimensional rectangular, periodic cell. These geometries provide an easy access to fast basis transforms by exploiting the periodicity of the basis functions, leading to FFT-based algorithms. Moreover, recent publications due to Temam et al. [7, 17, 22, 23] extend the idea of linear Galerkin approximations to nonlinear Galerkin methods. The key idea is that nonlinear expressions such as the nonlinear advection term can be treated more efficiently and also economically than in a linear Galerkin ansatz. Nonlinear Galerkin methods are able to capture the flow behavior with less test functions than that are needed within a linear Galerkin approach.

This article deals with a formulation of a nonlinear Galerkin method for solving the Navier-Stokes equations on the sphere involving vector and tensor spherical harmonics. The method itself is mainly motivated by the work of Marion and Temam [17] who have given a proof of convergence within a general Hilbert space concept. In detail, this work extends the results of [7, 22] from one-dimensional and toroidal domains to the spherical geometry, which is, for example, of great interest in meteorology and oceanography. Moreover, special emphasis is given on a fast computation of the nonlinear advection. Noteworthy, the techniques introduced later on differ from them used in the torus geometry due to the loss of periodicity in latitudinal direction. The idea is based on the so called *scalar pseudo spectral algorithms* or *transform methods* originally introduced by Orszag [19], see also related works of [2, 12, 24]. However, the main difference to [2, 12, 19, 24] is that the new method proposed below follows

---
*University of Kaiserslautern, Department of Mathematics, Geomathematics Group (fengler@mathematik.uni-kl.de, freeden@mathematik.uni-kl.de).

intrinsically a vectorial and tensorial formulation of the advection term. Thus, we are concerned with the fast transformation of (physically meaningful) vectorial and tensorial spherical harmonics which are not reduced (componentwise) to scalar ones. In doing so, we can easily separate the involved vector fields into poloidal and toroidal parts. This is of importance since we are interested here in flows, which are free of surface divergences. Finally, it should be noted that the term *transform method* is often used in meteorology to denote an exact variant of the so called *pseudo spectral method*, while the latter is then meant to be approximative (see, for instance, [19, 24]). However, throughout this work we follow the standard textbook of Boyd [3] and use the term *pseudo spectral method* synonymously, i.e., we use this method as an exact replacement of an algebraic evaluation of the advection term. In that sense, the term *pseudo spectral method* is understood to denote the general idea behind, which is applied to multiple other special functions and geometries, e.g., Chebyshev polynomials on finite intervals (see [3] and the references therein).

The layout of the paper is as follows: First, we introduce reference function spaces. Within this framework various estimates are derived, to show that the theorem of convergence as proposed by [17] can be applied. Second, we discuss the occurring coupling terms in the nonlinear Galerkin scheme, in particular the nonlinear advection term. To improve the algorithmic efficiency, we extend the techniques known for pseudo spectral algorithms to toroidal vector and tensor fields. Finally, we numerically illustrate our method for an extensive example, which involves the rotational Coriolis terms, the nonlinear advection, the viscosity, and the time-dependent flow driving forces.

2. Preliminaries. In what follows we adopt the nomenclature as proposed by Freeden, Gervens and Schreiner [11] in their monograph on *Constructive Approximation on the Sphere*:

$\mathbb{R}^3$ .... three dimensional Euclidean space
x, y, z .... elements of $\mathbb{R}^3$
$x \cdot y$ .... scalar product of vectors $x, y \in \mathbb{R}^3$
$x \wedge y$ .... vector product of vectors $x, y \in \mathbb{R}^3$
$x \otimes y$ .... tensor product of vectors $x, y \in \mathbb{R}^3$
$\varepsilon^i, i = 1, 2, 3$ .... canonical orthonormal basis in $\mathbb{R}^3$
∇ .... gradient in $\mathbb{R}^3$
Δ .... Laplacian in $\mathbb{R}^3$
r, t, ϕ .... polar coordinates in $\mathbb{R}^3$
Ω .... unit sphere in $\mathbb{R}^3$
ξ, η .... elements of the unit sphere $\Omega \subset \mathbb{R}^3$
$\varepsilon^r, \varepsilon^\phi, \varepsilon^t$ .... moving orthonormal triad on Ω
∇^* .... surface gradient on Ω
L^* .... surface curl gradient on Ω
$\nabla^* \cdot$ .... surface divergence on Ω
$L^* \cdot$ .... surface curl on Ω
Δ^* .... scalar Beltrami operator on Ω
$\boldsymbol{\Delta}^*$ .... vectorial Beltrami operator on Ω.

$C_{\mathbb{K}}^{(k)}(\Omega), L_{\mathbb{K}}^p(\Omega)$ (respectively $c_{\mathbb{K}}^{(k)}(\Omega), l_{\mathbb{K}}^p(\Omega)$) denote the following classes of scalar-valued (respectively, vector-valued) functions on Ω (with $\mathbb{K} = \mathbb{R}$ or $\mathbb{C}$):

$C_{\mathbb{K}}^{(k)}(\Omega)$ ...... class of scalar functions $F : \Omega \to \mathbb{K}$ possessing k continuous derivatives on Ω

$L_{\mathbb{K}}^{p}(\Omega)$ .... class of scalar functions $F : \Omega \to \mathbb{K}$ which are measurable and for which $\|F\|_{L^p(\Omega)} = (\int_{\Omega} |F(\xi)|^p dS(\xi))^{1/p} < \infty$ (dS is the surface element)

$c_{\mathbb{K}}^{(k)}(\Omega)$ ...... class of vector functions $f : \Omega \to \mathbb{K}^3$ possessing k continuous derivatives on Ω

$l_{\mathbb{K}}^{p}(\Omega)$ .... class of vector functions $f : \Omega \to \mathbb{K}^3$ which are measurable and for which $\|f\|_{l^p(\Omega)} = (\int_{\Omega} |f(\xi)|^p dS(\xi))^{1/p} < \infty$.

We denote by $Y_{n,k}$ the complex scalar spherical harmonics as introduced by Edmonds [8]. Moreover, we denote by $y_{n,k}^{(i)}(\xi)$ vector spherical harmonics for $n = 0_i, \ldots; k = -n, \ldots, n$ and $i = 1, 2, 3$, with $0_1 = 0$ and $0_2 = 0_3 = 1$. To be more specific, we let

$$y_{n,k}^{(1)}(\xi) = \xi Y_{n,k}(\xi),$$

$$y_{n,k}^{(2)}(\xi) = \frac{1}{\sqrt{n(n+1)}} \nabla_{\xi}^* Y_{n,k}(\xi),$$

$$y_{n,k}^{(3)}(\xi) = \frac{1}{\sqrt{n(n+1)}} L_{\xi}^* Y_{n,k}(\xi),$$

for $n = 0_i, \ldots; k = -n, \ldots, n$. Finally, the scalar spherical harmonics can be used to introduce tensor spherical harmonics by

$$\mathbf{y}_{n,k}^{(1,1)}(\xi) = \xi \otimes \xi Y_{n,k}(\xi), \qquad\qquad\qquad\qquad\qquad (2.1)$$

$$\mathbf{y}_{n,k}^{(1,2)}(\xi) = \frac{1}{\sqrt{n(n+1)}} \xi \otimes \nabla_{\xi}^* Y_{n,k}(\xi), \qquad \mathbf{y}_{n,k}^{(1,3)}(\xi) = \frac{1}{\sqrt{n(n+1)}} \xi \otimes L_{\xi}^* Y_{n,k}(\xi),$$

$$\mathbf{y}_{n,k}^{(2,1)}(\xi) = \frac{1}{\sqrt{n(n+1)}} \nabla_{\xi}^* Y_{n,k}(\xi) \otimes \xi, \qquad \mathbf{y}_{n,k}^{(2,2)}(\xi) = \frac{1}{\sqrt{n(n+1)}} \nabla_{\xi}^* \otimes \nabla_{\xi}^* Y_{n,k}(\xi),$$

$$\mathbf{y}_{n,k}^{(2,3)}(\xi) = \frac{1}{\sqrt{n(n+1)}} \nabla_{\xi}^* \otimes L_{\xi}^* Y_{n,k}(\xi), \qquad \mathbf{y}_{n,k}^{(3,1)}(\xi) = \frac{1}{\sqrt{n(n+1)}} L_{\xi}^* Y_{n,k}(\xi) \otimes \xi,$$

$$\mathbf{y}_{n,k}^{(3,2)}(\xi) = \frac{1}{\sqrt{n(n+1)}} L_{\xi}^* \otimes \nabla_{\xi}^* Y_{n,k}(\xi), \qquad \mathbf{y}_{n,k}^{(3,3)}(\xi) = \frac{1}{\sqrt{n(n+1)}} L_{\xi}^* \otimes L_{\xi}^* Y_{n,k}(\xi),$$

for $n = 0_{i,j}, \ldots; k = -n, \ldots, n$, with

$$0_{i,j} = \begin{cases} 0 & \text{if } (i,j) = (1,1), \\ 1 & \text{else.} \end{cases}$$

Furthermore, in analogy to [11], we introduce the function spaces:

$$\text{Harm}_{p,\ldots,q}(\Omega) = \text{span}_{n=p,\ldots,q; k=-n,\ldots,n}\{Y_{n,k}\}$$

$$\text{harm}_{p,\ldots,q}^{(i)}(\Omega) = \text{span}_{n=p,\ldots,q; k=-n,\ldots,n}\{y_{n,k}^{(i)}\}, \quad i = 1, 2, 3,$$

$$l_{(i)}^{2}(\Omega) = \overline{\text{harm}_{0_i,\ldots,\infty}^{(i)}(\Omega)}^{\|\cdot\|_{l^2(\Omega)}}.$$

From now on, we simply let $H = l_{(3)}^2(\Omega)$ if no confusion is likely to arise.

Finally, we introduce certain Sobolev spaces:

$$\mathcal{H}(\{A_n\}; \Omega) = \left\{ F \in L^2(\Omega) \Big| \sum_{n=0}^{\infty} \sum_{k=-n}^{n} \langle F, Y_{n,k} \rangle^2_{L^2(\Omega)} A_n^2 < \infty \right\},$$

$$h^{(i)}(\{A_n\}; \Omega) = \left\{ f \in l^2(\Omega) \Big| \sum_{n=0_i}^{\infty} \sum_{k=-n}^{n} \langle f, y_{n,k}^{(i)} \rangle^2_{l^2(\Omega)} A_n^2 < \infty \right\},$$

$$h(\{A_n\}; \Omega) = h^{(1)}(\{A_n\}; \Omega) \oplus h^{(2)}(\{A_n\}; \Omega) \oplus h^{(3)}(\{A_n\}; \Omega),$$

for sequences $\{A_n\}$ with $A_n \in \mathbb{R}$ for all n.

Following the terminology of [17], we let $A = -\boldsymbol{\Delta}^*$, i.e., A is the negative vectorial Beltrami operator. This basic dissipative operator A is a linear self-adjoint unbounded operator in H with domain of definition $D(A)$ dense in H (see [11]). Moreover, we know from [11] that A is positive and that A^{-1} is compact. Thus, one can define powers A^s of A for $s \in \mathbb{R}$; A^s maps $D(A^s)$ into H and $D(A^s)$ is a Sobolev space when endowed with the norm $\|A^s \cdot \|_{l^2_{(\Omega)}}$. We set $\mathcal{V} = D(A^{1/2})$, and denote by

$$\| \cdot \|_{\mathcal{V}} = \|(-\boldsymbol{\Delta}^*)^{1/2} \cdot \|_{l^2(\Omega)}$$

the norm on $\mathcal{V}$. Hence, we find by [11] the relation

$$\mathcal{V} = h^{(3)}(\{\sqrt{n(n+1)}\}; \Omega).$$

Thus we arrive at

$$A : H \supset D(A) \to H, \qquad u \mapsto Au = -\boldsymbol{\Delta}^* u. \qquad (2.2)$$

Moreover, we define the bilinear advection operator B by

$$B : \mathcal{V} \times \mathcal{V} \to \mathcal{V}', \qquad (u,v) \mapsto ((u \cdot \nabla^*)v), \qquad (2.3)$$

where $\mathcal{V}'$ is understood to be the dual space of $\mathcal{V}$. The Coriolis operator C is defined by

$$C : H \to H, \qquad u \mapsto 2\omega \wedge u, \qquad (2.4)$$

where ω denotes the rotational axis pointing in direction of ε^3. By $b(u,v,w) = \langle B(u,v), w \rangle_{\mathcal{V}',\mathcal{V}}$ we denote the trilinear form defined by

$$b(u,v,w) = \int_{\Omega} ((u \cdot \nabla^*)v) \cdot w \, dS, \qquad (2.5)$$

for all $u, v, w \in \mathcal{V}$. Finally, we introduce the space

$$L^2_{\Omega}(0, T; \mathcal{V}) = \left\{ f(t) \in \mathcal{V} : [0, T] \to \mathbb{R}^3 \left| \left(\int_0^T |f(t)|^2 \, dt \right)^{1/2} < \infty \right. \right\}.$$

The Navier-Stokes Equations: Throughout this work we denote by u the fluid velocity, by T the temperature, by p the pressure, by g the apparent gravity, by ρ the fluid's density. Additional flow driving terms are given by f, whereas friction

and dissipation is induced by a viscous term $\nu\Delta^*$. In the sense of meteorology, we introduce Q as the total heating rate per unit mass; c_v as the specific heat at constant volume, and c_R as the gas constant per unit mass. From [18] we recapitulate the set of forecasting equations for a pure tangential, atmospherical stream as follows:

$$\frac{\partial u}{\partial t} = -(u \cdot \nabla^*)u - 2\omega \wedge u - 1/\rho\nabla^*p - \nabla^*g + \nu\mathbf{\Delta}^*u + f \tag{2.6}$$

$$c_v\frac{\partial T}{\partial t} = -c_v(u \cdot \nabla^*)T - \frac{p}{\rho}\nabla^* \cdot u + Q \tag{2.7}$$

$$\frac{\partial \rho}{\partial t} = -(u \cdot \nabla^*)\rho - \rho\nabla^* \cdot u \tag{2.8}$$

$$p = \rho c_R T \tag{2.9}$$

$$u(0) = u_0, \qquad p(0) = p_0, \qquad T(0) = T_0, \qquad \rho(0) = \rho_0. \tag{2.10}$$

We restrict ourselves to pure tangential *incompressible* flows on a sphere. This leads us to $\nabla^* \cdot u = 0$ and $\rho = const.$, which simplifies (2.6)-(2.10). To be more specific, in our Galerkin approach, the pressure and gravity terms drop out in a weak formulation. Namely, let ϕ be a smooth toroidal vector-valued function, then

$$\langle \nabla^*p(t), \phi \rangle_{l^2(\Omega)} = 0$$

(by standard theorems, see, for example, [11]). The latter decouples the system (2.6)-(2.10), such that we have to consider "only" (in the weak sense) the equations

$$\frac{\partial u}{\partial t} = -(u \cdot \nabla^*)u - 2\omega \wedge u + \nu\mathbf{\Delta}^*u + f \tag{2.11}$$
$$\nabla^* \cdot u = 0$$
$$u(0) = u_0.$$

In the formulation used above, we can write (2.11) as follows

$$\frac{\partial u}{\partial t} + \nu Au + B(u, u) + Cu - f = 0, \tag{2.12}$$

where f is understood to be projected onto $l^2_{(3)}(\Omega)$.

Existence and Uniqueness: Il'in and Filatov [13, 14] have verified for the Navier-Stokes equations on the 2-sphere existence and uniqueness of a generalized (weak) solution, provided that $f \in L^2_\Omega(0, T; \mathcal{V}')$ and $u_0 \in H$. Moreover, they have proven that the solution is continuous and a member of class $L^2_\Omega(0, T; \mathcal{V})$.

3. Operator Estimates. This section is concerned with some operator estimates involving (2.12). Based on these results we are able to assure the convergence of the nonlinear Galerkin method. As a matter of fact, we present the estimates for the spherical case in the same way which is indicated by [17]. It should be noted that $l^2(\Omega)$ is written instead of $l^2_{\mathbb{R}}(\Omega)$ if no confusion is likely to arise.
First some results are borrowed from [14].

LEMMA 3.1 (Antisymmetry of the Trilinear Form). *For all $u, v, w \in \mathcal{V}$ the trilinear form b defined by (2.5) is antisymmetric, i.e.,*

$$b(u, v, w) = -b(u, w, v).$$

LEMMA 3.2. *For all* $u \in \mathcal{V}$

$$\|u\|_{l^4(\Omega)} \leq c_1 \|u\|_{l^2(\Omega)}^{1/2} \|u\|_{\mathcal{V}}^{1/2}. \tag{3.1}$$

From [10] we have the following important embedding theorem.

LEMMA 3.3 (Embedding $\mathcal{V}$). *Let* $2 \leq p \leq 4$. *Then*
  (i) $\mathcal{H}(\{n(n+1)\};\Omega) \subset \mathcal{H}(\{\sqrt{n(n+1)}\};\Omega) \subset L^p(\Omega) \subset L^2(\Omega)$,
  (ii) $h(\{n(n+1)\};\Omega) \subset h(\{\sqrt{n(n+1)}\};\Omega) \subset l^p(\Omega) \subset l^2(\Omega)$,
  (iii) $h^{(3)}(\{n(n+1)\};\Omega) \subset h^{(3)}(\{\sqrt{n(n+1)}\};\Omega) \subset l_{(3)}^p(\Omega) \subset l_{(3)}^2(\Omega)$,
  (iv) $\mathcal{V} \subset l_{(3)}^p(\Omega) \subset l_{(3)}^2(\Omega)$.

Consequently, we can deduce a corollary relating the norms of the involved Sobolev spaces and $l^2(\Omega)$.

COROLLARY 3.4. *Assume that* u *is real valued and of class* $h^{(3)}(\{n(n+1)\};\Omega)$. *Then*

$$\|u\|_{l^2(\Omega)} \leq \|u\|_{\mathcal{V}} \leq \|u\|_{h^{(3)}(\{n(n+1)\};\Omega)}.$$

Based on these results we are able to deduce the following estimates:

ESTIMATE 3.5 (Estimating the Trilinear Form). *The trilinear form* b *can be estimated for all* $u, v, w \in \mathcal{V}$ *by*
  (i)

$$|b(u,v,w)| \leq c_1 \|u\|_{\mathcal{V}} \|v\|_{\mathcal{V}} \|w\|_{\mathcal{V}},$$

  (ii)

$$|b(u,v,w)| \leq c_2 \|u\|_{l^2(\Omega)}^{1/2} \|u\|_{\mathcal{V}}^{1/2} \|v\|_{\mathcal{V}} \|w\|_{l^2(\Omega)}^{1/2} \|w\|_{\mathcal{V}}^{1/2}. \tag{3.2}$$

Proof. The first statement has already been proven in [14].

The second statement can be derived by expanding the trilinear form in its cartesian components: By keeping in mind that u, v, w are tangential vector fields, we find

$$b(u,v,w) = \int_\Omega [(u \cdot \nabla^*)v] \cdot w \; dS = \int_\Omega [(u \cdot \nabla)v] \cdot w \; dS. \tag{3.3}$$

Since ∇ is the gradient in $\mathbb{R}^3$, we are able to expand (3.3) componentwise in cartesian coordinates, i.e., $v_i = \varepsilon^i \cdot v$, and $\nabla_i = \varepsilon^i \cdot \nabla$, such that

$$b(u,v,w) = \int_\Omega \sum_{i=1}^3 \sum_{j=1}^3 u_i (\nabla_i v_j) w_j \; dS.$$

By applying twice Cauchy-Schwarz we estimate the absolute value of b by

$$|b(u,v,w)| \leq \sum_{i=1}^3 \sum_{j=1}^3 \int_\Omega |u_i(\nabla_i v_j)w_j| \; dS \leq \sum_{i=1}^3 \sum_{j=1}^3 \|u_i\|_{L^4(\Omega)} \|\nabla_i v_j\|_{L^2(\Omega)} \|w_j\|_{L^4(\Omega)}$$

$$\leq \left(\sum_{i=1}^3 \|u_i\|_{L^4(\Omega)}\right)^{1/2} \left[\sum_{j=1}^3 \left(\sum_{i=1}^3 \|\nabla_i v_j\|_{L^2(\Omega)}\right)^{1/2} \|w_j\|_{L^4(\Omega)}\right] \tag{3.4}$$

$$\leq \left(\sum_{i=1}^3 \|u_i\|_{L^4(\Omega)}\right)^{1/2} \left(\sum_{i=1}^3 \sum_{j=1}^3 \|\nabla_i v_j\|_{L^2(\Omega)}\right)^{1/2} \left(\sum_{j=1}^3 \|w_j\|_{L^4(\Omega)}\right)^{1/2}.$$

Now the first and third sum can be estimated by aid of (3.1)

$$\|u_i\|_{L^4(\Omega)}^2 = \|u_i \varepsilon_i\|_{l^4(\Omega)}^2 \leq \|u\|_{l^4(\Omega)}^2 \leq c_1^2 \|u\|_{l^2(\Omega)} \|u\|_{\mathcal{V}}.$$

This leads us to

$$\left(\sum_{i=1}^{3} \|u_i\|_{L^4(\Omega)}^2 \right)^{1/2} \leq \sqrt{3} c_1 \|u\|_{l^2(\Omega)}^{1/2} \|u\|_{\mathcal{V}}^{1/2}. \tag{3.5}$$

Observing the estimate

$$\sum_{i=1}^{3} \sum_{j=1}^{3} \|\nabla_i v_j\|_{L^2(\Omega)}^2 = \sum_{i=1}^{3} \sum_{j=1}^{3} \int_{\Omega} \nabla_i v_j \nabla_i v_j \, dS = -\sum_{i=1}^{3} \sum_{j=1}^{3} \int_{\Omega} v_j (\nabla_i)^2 v_j \, dS$$

$$= -\sum_{i=1}^{3} \int_{\Omega} v \cdot (\nabla_i)^2 v \, dS = -\int_{\Omega} v \cdot \Delta v \, dS$$

$$= -\int_{\Omega} v \cdot \Delta^* v \, dS = \|v\|_{\mathcal{V}}^2$$

we finally get the desired result. □
In the following we are concerned with the well known Poincaré inequality on the sphere.

ESTIMATE 3.6 (Poincaré Inequality). *Assume that $u \in \mathcal{V}$. Then*

$$\|u\|_{l^2(\Omega)} \leq \frac{1}{\sqrt{2}} \|u\|_{\mathcal{V}}.$$

Proof. Let us expand u in type 3 vector spherical harmonics, such that $u = \sum_{n=1}^{\infty} u_{n,k}^{(3)} y_{n,k}^{(3)}$. Then $\|u\|_{\mathcal{V}}^2$ reads as

$$\|u\|_{\mathcal{V}}^2 = \sum_{n=1}^{\infty} n(n+1) \left(u_{n,k}^{(3)} \right)^2.$$

Since $n(n+1) \geq 2$, for all $n \geq 1$ we get the desired result. □

ESTIMATE 3.7 (Estimating the Coriolis Term). *For $u \in \mathcal{V}$, and $\omega \in \mathbb{R}^3$*

$$\|Cu\|_{l^2(\Omega)} \leq \sqrt{2} |\omega| \|u\|_{\mathcal{V}}.$$

Proof. First we see that

$$\|Cu\|_{l^2(\Omega)} \leq 2 \|\omega \wedge u\|_{l^2(\Omega)} = 2 \left[\int_{\Omega} (\omega \wedge u)^2 \, dS \right]^{1/2}.$$

Applying the Lagrange identity we obtain

$$2 \left[\int_{\Omega} (\omega \wedge u)^2 \, dS \right]^{1/2} = 2 \left[\int_{\Omega} (\omega \cdot \omega)(u \cdot u) - (u \cdot \omega)(\omega \cdot u) \, dS \right]^{1/2}$$

$$\leq 2 \left[\int_{\Omega} |\omega|^2 (u \cdot u) \, dS \right]^{1/2} = 2 |\omega| \|u\|_{l^2(\Omega)}.$$

By aid of the Poincaré inequality from Estimate 3.6 we have

$$2|\omega|\|u\|_{l^2(\Omega)} \leq \sqrt{2}|\omega|\|u\|_{\mathcal{V}},$$

which proves our estimate. □

ESTIMATE 3.8 (Positive Definiteness of $\nu A + C$). *Let A be the vectorial Stokes operator from (2.2), and C the Coriolis operator from (2.4). For $\nu \in \mathbb{R}^+$ and $u \in \mathcal{V}$*

$$\int_\Omega [(\nu A + C)u] \cdot u \, dS \geq \nu\|u\|_{\mathcal{V}}^2.$$

Proof. Let us drop for a moment the operator νA. We expand u in type 3 vector spherical harmonics, such that $u = \sum_{n=1}^\infty \sum_{k=-n}^n u_{n,k}^{(3)} y_{n,k}^{(3)}$ in the sense of $l^2(\Omega)$. Then, we get for the Coriolis operator the following identity

$$\int_\Omega Cu \cdot u \, dS = 2 \int_\Omega (\omega \wedge u) \cdot u \, dS = 0.$$

By using the linearity of the integral operator, we are able to deduce that

$$\int_\Omega [(\nu A + C)u] \cdot u \, dS = \int_\Omega \nu Au \cdot u \, dS = \nu\|u\|_{\mathcal{V}}^2.$$

This guarantees Estimate 3.8. □

Finally we are concerned with some estimates for the nonlinear advection operator B.

ESTIMATE 3.9 (Estimating the Advection Operator). *If B denotes the nonlinear advection operator defined by (2.3) then we have the following inequalities:*

(i) *Suppose that $v \in D(A), u \in \mathcal{V}$. Then*

$$\|B(u,v)\|_{l^2(\Omega)} \leq c_2\|u\|_{l^2(\Omega)}^{1/2}\|u\|_{\mathcal{V}}^{1/2}\|v\|_{\mathcal{V}}^{1/2}\|Av\|_{l^2(\Omega)}^{1/2}. \tag{3.6}$$

(ii) *For all $u \in D(A)$ we have*

$$\|B(u,u)\|_{l^2(\Omega)} \leq c_2\|u\|_{l^2(\Omega)}^{1/2}\|u\|_{\mathcal{V}}\|Au\|_{l^2(\Omega)}^{1/2}.$$

(iii) *Let $v \in D(A), u \in \mathcal{V}$. Then*

$$\|B(u,v)\|_{\mathcal{V}'} \leq c_2\|u\|_{l^2(\Omega)}^{1/2}\|u\|_{\mathcal{V}}^{1/2}\|v\|_{\mathcal{V}}^{1/2}\|v\|_{l^2(\Omega)}^{1/2}.$$

(iv) *For all $u, v \in D(A)$ we have*

$$\|B(u,v)\|_{\mathcal{V}'} \leq c_2\|u\|_{l^2(\Omega)}^{1/2}\|u\|_{\mathcal{V}}\|v\|_{\mathcal{V}}^{1/2}.$$

(v) *For all $u, v \in D(A)$ we have*

$$\|B(u,v)\|_{l^2(\Omega)} \leq c_2\|u\|_{l^2(\Omega)}^{1/2}\|u\|_{\mathcal{V}}\|v\|_{\mathcal{V}}^{1/2}.$$

(vi) *For all $u, v \in D(A)$ we have*

$$\|B(u,v)\|_{l^2(\Omega)} \leq c_2\|u\|_{\mathcal{V}}^{1/2}\|Au\|_{l^2(\Omega)}^{1/2}\|v\|_{\mathcal{V}}.$$

Before entering detailed steps for the proof of these five estimates we need a preliminary result:

LEMMA 3.10. *Suppose that* $v \in h^{(3)}(\{A_n\}; \Omega) \subset l^2_{(3)}(\Omega)$, *where* $\{A_n\}$ *is an admissible sequence. Then*

$$\|v \cdot \varepsilon_i\|_{\mathcal{H}(\{A_n\}; \Omega)} \leq \|v\|_{h(\{A_n\}; \Omega)}$$

for all i=1,2,3.

Proof. It is clear that $\|v \cdot \varepsilon_i\|_{L^2(\Omega)} \leq \|v\|_{l^2(\Omega)}$. As $y^{(3)}_{n,k} \in \oplus^3_{i=1} \mathrm{Harm}_n(\Omega) \varepsilon_i$, for all $k = -n, \ldots, n$, (see [11]). Since $v \in l^2_{(3)}(\Omega)$ we are able to verify that

$$\sum^n_{k=-n} \left\langle v, y^{(3)}_{n,k} \right\rangle_{l^2(\Omega)} y^{(3)}_{n,k} = \sum^3_{i=1} \sum^n_{k=-n} \langle v, Y_{n,k} \varepsilon_i \rangle_{l^2(\Omega)} Y_{n,k} \varepsilon_i.$$

From the right hand side we get an estimate for the Fourier coefficients of the component functions $v_i, i = 1, 2, 3$:

$$\sum^n_{k=-n} |(v \cdot \varepsilon_i)^\wedge(n,k)|^2 \leq \sum^3_{i=1} \sum^n_{k=-n} |(v \cdot \varepsilon_i)^\wedge(n,k)|^2 = \sum^n_{k=-n} |v^{(3)}(n,k)|^2.$$

By similar arguments we obtain

$$A^2_n \sum^n_{k=-n} |(v \cdot \varepsilon_i)^\wedge(n,k)|^2 \leq A^2_n \sum^n_{k=-n} |v^{(3)}(n,k)|^2$$
$$\|v \cdot \varepsilon_i\|_{\mathcal{H}(\{A_n\}; \Omega)} \leq \|v\|_{h(\{A_n\}; \Omega)}.$$

☐

Lemma 3.3 and 3.10 enable us to establish the proof of Estimate 3.9.

Proof.
(i) The first estimate can be derived from (3.4) and (3.5):

$$|b(u,v,w)| \leq \left(\sum^3_{i=1} \|u_i\|_{L^4(\Omega)} \right)^{1/2} \left(\sum^3_{i=1} \sum^3_{j=1} \|\nabla_i v_j\|_{L^2(\Omega)} \right)^{1/2} \left(\sum^3_{j=1} \|w_j\|_{L^4(\Omega)} \right)^{1/2}$$

$$\leq \left(\sum^3_{i=1} \sum^3_{j=1} \|\nabla_i v_j\|_{L^2(\Omega)} \right)^{1/2} \sqrt{3} c_1 \|u\|^{1/2}_{l^2(\Omega)} \|u\|^{1/2}_{\mathcal{V}} \|w\|_{l^2(\Omega)}. \qquad (3.7)$$

It remains to look at the first term. Due to our assumption we have $v \in D(A) \subset h(\{n(n+1)\}; \Omega)$. Thus, $\nabla_i v_j \in \mathcal{H}(\{\sqrt{n(n+1)}\}; \Omega) \subset L^4(\Omega) \subset L^2(\Omega)$ by aid of Lemma 3.3. This yields $\|\nabla_i v_j\|_{L^2(\Omega)} \leq \|\nabla_i v_j\|_{L^4(\Omega)}$. We observe

$$\|\nabla_i v_j\|^4_{L^4(\Omega)} = \|(\varepsilon_i \cdot \nabla) v_j\|^4_{L^4(\Omega)} \leq \|\nabla v_j\|^4_{l^4(\Omega)} \leq c^4_1 \|\nabla v_j\|^2_{l^2(\Omega)} \|\nabla v_j\|^2_{\mathcal{V}}. \qquad (3.8)$$

The term on the right-hand side of (3.8) can be further simplified by

$$\|\nabla v_j\|^4_{l^4(\Omega)} \leq c^4_1 \|\nabla^* v_j\|^2_{l^2(\Omega)} \|\nabla^* v_j\|^2_{\mathcal{V}} = c^4_1 \|v_j\|^2_{\mathcal{V}} \|\Delta^* v_j\|^2_{L^2(\Omega)}.$$

By using the auxiliary Lemma 3.10 we get

$$\|\nabla_i v_j\|_{L^4(\Omega)}^4 \le c_1^4 \|v\|_{\mathcal{V}}^2 \|\Delta^* v\|_{l^2(\Omega)}^2 = c_1^4 \|v\|_{\mathcal{V}}^2 \|Av\|_{l^2(\Omega)}^2.$$

Taking the fourth root of both sides of the equation yields

$$\|\nabla_i v_j\|_{L^4(\Omega)} \le c_1 \|v\|_{\mathcal{V}}^{1/2} \|Av\|_{l^2(\Omega)}^{1/2}.$$

By plugging the last result into (3.7) we find

$$|b(u,v,w)| \le 3\sqrt{3}c_1^2 \|u\|_{l^2(\Omega)}^{1/2} \|u\|_{\mathcal{V}}^{1/2} \|v\|_{\mathcal{V}}^{1/2} \|Av\|_{l^2(\Omega)}^{1/2} \|w\|_{l^2(\Omega)}.$$

Finally we can conclude the first estimate for the advection operator B

$$\|B(u,v)\|_{l^2(\Omega)} = \sup_{w \in H} \frac{\langle B(u,v), w\rangle_{l^2(\Omega)}}{\|w\|_{l^2(\Omega)}} = \sup_{w \in H} \frac{|b(u,v,w)|}{\|w\|_{l^2(\Omega)}}$$
$$\le 3\sqrt{3}c_1^2 \|u\|_{l^2(\Omega)}^{1/2} \|u\|_{\mathcal{V}}^{1/2} \|v\|_{\mathcal{V}}^{1/2} \|Av\|_{l^2(\Omega)}^{1/2}.$$

(ii) The second estimate follows from the first one by setting $v = u$.

(iii) To verify the third estimate we use the estimate from (3.2)

$$|b(u,v,w)| \le c_2 \|u\|_{l^2(\Omega)}^{1/2} \|u\|_{\mathcal{V}}^{1/2} \|v\|_{\mathcal{V}} \|w\|_{l^2(\Omega)}^{1/2} \|w\|_{\mathcal{V}}^{1/2} \tag{3.9}$$

and use the antisymmetry relation for the trilinear form b from Lemma 3.1, i.e., $b(u,v,w) = -b(u,w,v)$, to deduce that

$$|b(u,v,w)| \le c_2 \|u\|_{l^2(\Omega)}^{1/2} \|u\|_{\mathcal{V}}^{1/2} \|w\|_{\mathcal{V}} \|v\|_{l^2(\Omega)}^{1/2} \|v\|_{\mathcal{V}}^{1/2}.$$

By keeping in mind the Riesz-Fischer representation theorem we may regard for all $u \in \mathcal{V}$ and $v \in D(A)$ the value $B(u,v)$ as a representation of a linear functional in $\mathcal{V}'$. Thus we can estimate the norm of this functional by

$$\|B(u,v)\|_{\mathcal{V}'} = \sup_{w \in \mathcal{V}} \frac{|\langle B(u,v), w\rangle_{l^2(\Omega)}|}{\|w\|_{\mathcal{V}}} = \sup_{w \in \mathcal{V}} \frac{|b(u,v,w)|}{\|w\|_{\mathcal{V}}}$$
$$\le c_2 \|u\|_{l^2(\Omega)}^{1/2} \|u\|_{\mathcal{V}}^{1/2} \|v\|_{l^2(\Omega)}^{1/2} \|v\|_{\mathcal{V}}^{1/2}$$

which finally proves the third estimate.

(iv) The proof of this estimate follows directly from the relation (iii) and (3.9), i.e.,

$$\|B(u,v)\|_{\mathcal{V}'} = \sup_{\|w\|_{\mathcal{V}}=1} |b(u,v,w)| \le \sup_{\|w\|_{\mathcal{V}}=1} c_2 \|u\|_{l^2(\Omega)}^{1/2} \|u\|_{\mathcal{V}}^{1/2} \|v\|_{\mathcal{V}} \|w\|_{l^2(\Omega)}^{1/2} \|w\|_{\mathcal{V}}^{1/2}.$$

Since $\|w\|_{l^2(\Omega)} \le \|w\|_{\mathcal{V}}$ from the Poincaré inequality we finally arrive at

$$\|B(u,v)\|_{\mathcal{V}'} \le c_2 \|u\|_{l^2(\Omega)}^{1/2} \|u\|_{\mathcal{V}}^{1/2} \|v\|_{\mathcal{V}}.$$

(v) The fifth estimate can easily be obtained from (iv) by applying again the Riesz-Fischer representation theorem. This theorem yields the identity $\|B(u,v)\|_{\mathcal{V}'} = \|B(u,v)\|_{\mathcal{V}}$. From $\|B(u,v)\|_{l^2(\Omega)} \le \|B(u,v)\|_{\mathcal{V}}$ we get the desired result.

(vi) The last estimate can be derived by using again (3.2). The Poincaré inequality yields

$$\|B(u,v)\|_{l^2(\Omega)} \le \|B(u,v)\|_{\mathcal{V}} = \|B(u,v)\|_{\mathcal{V}'}$$

$$\le \sup_{\|w\|_{\mathcal{V}}=1} c_2\|u\|_{l^2(\Omega)}^{1/2}\|u\|_{\mathcal{V}}^{1/2}\|v\|_{\mathcal{V}}\|w\|_{l^2(\Omega)}^{1/2}\|w\|_{\mathcal{V}}^{1/2}$$

$$\le \sup_{\|w\|_{\mathcal{V}}=1} c_2\|u\|_{l^2(\Omega)}^{1/2}\|u\|_{\mathcal{V}}^{1/2}\|v\|_{\mathcal{V}}\|w\|_{\mathcal{V}}$$

$$\le c_2\|u\|_{l^2(\Omega)}^{1/2}\|u\|_{\mathcal{V}}^{1/2}\|v\|_{\mathcal{V}}.$$

Since we required $u \in D(A) \subset h^{(3)}(\{n(n+1)\}; \Omega)$, we obtain the result by Corollary 3.4

$$\|B(u,v)\|_{l^2(\Omega)} \le c_2\|u\|_{h^{(3)}(\{n(n+1)\};\Omega)}^{1/2}\|u\|_{\mathcal{V}}^{1/2}\|v\|_{\mathcal{V}} = c_2\|Au\|_{l^2(\Omega)}^{1/2}\|u\|_{\mathcal{V}}^{1/2}\|v\|_{\mathcal{V}}.$$

☐

4. The Nonlinear Galerkin Method on the Sphere. The implementation of the Galerkin method is based on the set of eigenvectors $\{y_{n,k}^{(3)}\}, n = 1, \ldots; k = -n, \ldots, n$, of the operator A with eigenvalues $0 < n(n+1), n = 1, 2, \ldots$. Further, for $m \in \mathbb{N}$, we consider the spaces $\mathrm{harm}_{1,\ldots,m}^{(3)}(\Omega)$ and $\mathrm{harm}_{m+1,\ldots,2m}^{(3)}(\Omega)$, respectively. Moreover, let $P_{1,\ldots,m}$ be the orthogonal projection operator $P_{1,\ldots,m} : l^2(\Omega) \to \mathrm{harm}_{1,\ldots,m}^{(3)}(\Omega)$, respectively $P_{m+1,\ldots,2m}$ the projector on $\mathrm{harm}_{m+1,\ldots,2m}^{(3)}(\Omega)$.

Assume that u_0 is of class H, and let u be the solution of (2.12) with the initial condition $u(0) = u_0$. For every integer m, we are now looking for an approximation u_m of the form

$$u_m : \mathbb{R}_0^+ \to \mathrm{harm}_{1,\ldots,m}^{(3)}(\Omega), \qquad u_m(t) = \sum_{n=1}^{m} \sum_{k=-n}^{n} u_{n,k}^m(t) y_{n,k}^{(3)}. \tag{4.1}$$

The function u_m is determined by the resolution of a system involving another unknown function z_m, given by

$$z_m : \mathbb{R}_0^+ \to \mathrm{harm}_{m+1,\ldots,2m}^{(3)}(\Omega), \qquad z_m(t) = \sum_{n=m+1}^{2m} \sum_{k=-n}^{n} z_{n,k}^m(t) y_{n,k}^{(3)}. \tag{4.2}$$

The pair (u_m, z_m) is expected to fulfill the equations

$$\frac{\partial}{\partial t}\langle u_m, v\rangle_{l^2(\Omega)} + \nu\langle Au_m, v\rangle_{l^2(\Omega)} + \langle Cu_m, v\rangle_{l^2(\Omega)} + b(u_m, u_m, v) \tag{4.3}$$

$$+ b(z_m, u_m, v) + b(u_m, z_m, v) = \langle f, v\rangle_{l^2(\Omega)},$$

$$\nu\langle Az_m, \tilde{v}\rangle_{l^2(\Omega)} + \langle Cz_m, \tilde{v}\rangle_{l^2(\Omega)} + b(u_m, u_m, \tilde{v}) = \langle f, \tilde{v}\rangle_{l^2(\Omega)}, \tag{4.4}$$

for all $v \in \mathrm{harm}_{1,\ldots,m}^{(3)}(\Omega)$ and $\tilde{v} \in \mathrm{harm}_{m+1,\ldots,2m}^{(3)}(\Omega)$, together with

$$u_m(0) = P_{1,\ldots,m}u_0. \tag{4.5}$$

Our purpose is to show that the system (4.3) and (4.4) is equivalent to an ordinary differential equation in terms of u_m:

Observing that $P_{m+1,\ldots,2m}Az_m = Az_m$ (4.4) is indeed linear in z_m, hence, can be written as

$$(\nu A + P_{m+1,\ldots,2m}C)z_m = P_{m+1,\ldots,2m}(f - B(u_m, u_m)). \qquad (4.6)$$

By virtue of Estimate 3.8, [17] guarantees the invertibility of the projected operator $P_{m+1,\ldots,2m}(\nu A + C)$ on $\mathrm{harm}^{(3)}_{m+1,\ldots,2m}(\Omega)$. Therefore, we have z_m explicitly given in terms of u_m by

$$z_m = (\nu A + P_{m+1,\ldots,2m}C)^{-1}P_{m+1,\ldots,2m}(f - B(u_m, u_m)). \qquad (4.7)$$

Then, the system (4.3), (4.4) is equivalent to the ordinary differential system

$$\frac{\partial u_m}{\partial t} + \nu A u_m + P_{1,\ldots,m}(Cu_m + B(u_m, u_m) + B(z_m, u_m) + B(u_m, z_m)) = P_{1,\ldots,m}f, \quad (4.8)$$

with z_m given by (4.7).

Note that the system (4.8) with $z_m = 0$ yields exactly as a byproduct the linear Galerkin method on the sphere.

Existence and uniqueness of a solution u_m to the system (4.8) equipped with the initial value from (4.5) defined on a maximal interval $[0, T_{\max})$ follows from standard theorems on ordinary differential equations. In fact, it is known that $T_{\max} = +\infty$ (see, for example, [17]). Based on all results stated above, we can study now the limit $m \to +\infty$:

THEOREM 4.1 (Main Convergence Theorem). *By virtue of Lemma 3.1 and the Estimates 3.5, 3.7, 3.9 the solution u_m of the ordinary differential equation (4.8) with the initial value (4.5) converges, as $m \to +\infty$, to the solution u of the spherical Navier-Stokes equation (2.12) with the initial value $u(0) = u_0$ with $u_0 \in H$ in the following sense:*

- $u_m \to u$ *in* $L^2(0, T; \mathcal{V})$ *and* $L^p(0, T; H)$ *strongly, for all* $T > 0$ $\qquad$ (4.9) *and all* $1 \leq p < \infty$;
- $u_m \to u$ *in* $L^\infty(\mathbb{R}^+; H)$ *weak-star.*

The proof can be found in [17] for a general Hilbert space concept. It outlines the intuition that on the one hand z_m is small compared to u_m, but on the other hand, that, at each given time, $z_m(t)$ is a minor correction to $u_m(t)$. Moreover, it turns out, that on long intervals of times, z_m modifies u_m in a non-negligible way.

5. Implementation of the Nonlinear Galerkin Scheme. Referring to (4.3) and (4.4) we formulate here an algorithm based on an Euler method, for the sake of clarity. However, it should be outlined that we use in our numerical implementation an explicit Runge-Kutta-4(5) method.

ALGORITHM 5.1 (Nonlinear Galerkin Scheme (Euler Variant)).
Purpose: *Compute an approximation $u_m(t)$, $t \in [t_0, T]$, for some $T > t$ based on an Euler scheme. Let u_0 be the initial value, i.e., $u_0 = u(t_0) \in H$. Moreover, $t_i = t_0 + ih$ be the time-step, with some time-stepping size $h > 0$.*

while $t_i \leq T$

Compute $z_m = z_m(t_i)$ from $u_m = u_m(t_i)$ and $f = f(t_i)$, by solving the linear system

$$\nu \left\langle Az_m, y_{n,j}^{(3)} \right\rangle_{l^2(\Omega)} + \left\langle Cz_m, y_{n,j}^{(3)} \right\rangle_{l^2(\Omega)} + \left\langle B(u_m, u_m), y_{n,j}^{(3)} \right\rangle_{l^2(\Omega)} \tag{5.1}$$

$$= \left\langle f, y_{n,j}^{(3)} \right\rangle_{l^2(\Omega)}$$

for $n = m + 1, \ldots, 2m; j = -n, \ldots, n$. Compute $k = \sum_{n=1}^{m} \sum_{j=-n}^{n} k_{n,j}^{(3)} y_{n,j}^{(3)}$ by solving the linear system for the Fourier coefficients:

$$\left\langle k, y_{n,j}^{(3)} \right\rangle_{l^2(\Omega)} = \left\langle f, y_{n,j}^{(3)} \right\rangle_{l^2(\Omega)} - \nu \left\langle Au_m, y_{n,j}^{(3)} \right\rangle_{l^2(\Omega)} - \left\langle Cu_m, y_{n,j}^{(3)} \right\rangle_{l^2(\Omega)} \tag{5.2}$$

$$- \left\langle B(u_m, u_m), y_{n,j}^{(3)} \right\rangle_{l^2(\Omega)} - \left\langle B(z_m, u_m), y_{n,j}^{(3)} \right\rangle_{l^2(\Omega)} \tag{5.3}$$

$$- \left\langle B(u_m, z_m), y_{n,j}^{(3)} \right\rangle_{l^2(\Omega)},$$

for $n = 1, \ldots, m; j = -n, \ldots, n$. Continue with the next step:

$$u_m(t_{i+1}) = u_m(t_i) + hk$$

end while

The above noted algorithm requires the computation of coupling integrals. The latter are of special interest in the case of the Coriolis term and the nonlinear advection. In [10] we find the following theorems, which are very cumbersome to establish by use of Wigner-$3j, -6j$ and $-9j$ symbols.

THEOREM 5.2 (Calculation of the Coriolis Term). *Let $k, l, n, j \in \mathbb{N}$ with $k > 0, r > 0$, $n > 0$, and $\omega = |\omega|\varepsilon^3$. Then,*

$$\int_{\Omega} (\omega \wedge y_{k,l}^{(3)}(\eta)) \cdot y_{n,j}^{(3)*}(\eta) \, dS(\eta) = |\omega| i \frac{-l}{n(n+1)} \delta_{k,n} \delta_{l,j}. \tag{5.4}$$

THEOREM 5.3 (Calculation of the Advection Term). *Let $k, l, n, j, r, s \in \mathbb{N}$ with $k > 0, r > 0$, and $n > 0$. Then,*

$$\int_{\Omega} [(y_{k,l}^{(3)}(\eta) \cdot \nabla_{\eta}^*) y_{r,s}^{(3)}(\eta)] \cdot y_{n,j}^{(3)*}(\eta) \, dS(\eta) = T(n, j, r, s, k, l), \tag{5.5}$$

where we have introduced the abbreviation

$$T(n, j, r, s, k, l) = (-1)^{j+1} i \frac{1}{\sqrt{4\pi}} \frac{n(n+1) + r(r+1) - k(k+1)}{4\sqrt{r(r+1)n(n+1)k(k+1)}}$$

$$\times \begin{pmatrix} r & n & k \\ s & -j & l \end{pmatrix} \sqrt{(2r+1)(2n+1)(2k+1)} \begin{pmatrix} r-1 & n & k \\ 0 & 0 & 0 \end{pmatrix}$$

$$\times \sqrt{(n+k+r+1)(k+r-n)(n-k+r)(n+k-r+1)}.$$

COROLLARY 5.4. *By using the Wigner-$3j$ properties we find that the coupling term in (5.5) vanishes, i.e.,*

$$\int_{\Omega} [(y_{k,l}^{(3)}(\eta) \cdot \nabla_{\eta}^*) y_{r,s}^{(3)}(\eta)] \cdot y_{n,j}^{(3)*}(\eta) \, dS(\eta) = 0$$

for the following three cases:

(i) $k > r + n$ or $k < |r - n|$,

(ii) $s + l - j \neq 0$,

(iii) $r + n + k$ is even.

Now we consider the nonlinear part in (5.1) in more detail by dropping for a moment all other terms. Expanding u in terms of type 3 vector spherical harmonics we are able to express the Fourier coefficients of z in connection of (5.5) by

$$\tilde{z}_{n,j} = \sum_{r=1}^{N} \sum_{s=-r}^{r} \sum_{k=1}^{N} \sum_{l=-k}^{k} u_{r,s}^{(3)} u_{k,l}^{(3)} T(n, j, r, s, k, l), \tag{5.6}$$

for $n = N + 1, \ldots, 2N; |j| \leq n$. Since our considered velocity field of the flow is real-valued, we can restrict the computation to all j with $0 \leq j \leq n$, and obtain all remaining coefficients for negative orders by anti-symmetry. To estimate the number of operations required to compute the coefficients $\tilde{z}_{n,j}$, we assume that the quantity T has been tabulated beforehand. By exploiting the Wigner-$3j$ selection rule from Corollary 5.4 (iii), we have a total of

$$\sum_{n=N+1}^{2N} (n + 1) \sum_{r=1}^{N} (2r + 1)^2 \approx 2N^5$$

complex×complex×real multiplications, each of them is equivalent to 6 real multiplications. Selection rules for $3j$-coefficients with zero bottom row, require $r - 1 + n + k$ to be even, reducing the number of terms in (5.6) by a factor of 2. Thus, the number of real multiplications is about $6N^5$. For each 6 real multiplications, (5.6) involves 2 real additions; and thus a total of about $2N^5$ additions.

Since values of N greater than 100 occur in practice (for example, in meteorology, the European Center for Medium-Range Forecast (ECMWF) uses N=511, see [21]), it is important to reduce the preceding estimate for the number of operations. Furthermore, the preceding estimate assumes that the coupling integrals have been tabulated in an a priori step. Although Wigner selection rules and symmetries greatly reduce the storage required, the number of storage locations scale like $O(N^5)$.

To improve the scaling for the evaluation of nonlinear terms several authors [2, 6, 12, 19, 15, 24] introduced FFT-techniques to evaluate these so called vector-coupled sums. The first seems to be Orszag [19] in 1970, whereas James [15] extended Orszag's method to his tensor calculus in 1974. For a detailed overview to pseudo spectral methods the reader is referred to Corey [6] and the references therein.

5.1. Fast Pseudo Spectral Algorithm. The extension of Orszag's method to spherical vector and tensor fields can be found by James [15] for his tensor calculus. Unfortunately, his rank-k-tensor approach differs in its basis representation from our philosophy: We like to separate any vector and tensor field in physically meaningful parts, e.g., into tangential and radial components, or to be more specific, into surface gradient and surface curl (toroidal) contributions etc.

Thus, this section is dedicated to the rapid evaluation of the nonlinear advection term $(u \cdot \nabla^*)u = (\nabla^* \otimes u)^T u$ involving the framework of vectorial and tensorial harmonics. The main advantage of our methods proposed in the following, is that they are based on *stable numerical* integration in the Gauss-Legendre-Transform (GLT)

rather than solving linear systems as proposed by James [15]. For a detailed description of the vectorial and tensorial variants, algorithms and examples see [10]. The techniques introduced now, allow us to evaluate and reconstruct the advection term in the order $O(N^3)$ instead of the estimate $O(N^5)$ explained above.

Idea: Before formulating the algorithm we sketch for brevity the idea of pseudo spectral methods in the vectorial type 3 case. Obviously the evaluation and reconstruction of real type 3 vector fields $u_N^{(3)} \in \operatorname{harm}_{1,\ldots,N}^{(3)}(\Omega)$ can be written out as follows:

$$u_N^{(3)} = \sum_{n=1}^{N} \sum_{k=-n}^{n} u_{n,k}^{(3)} y_{n,k}^{(3)}, \tag{5.7}$$

where

$$y_{n,k}^{(3)}(t,\phi) = \frac{(-1)^k}{\sqrt{n(n+1)}} \left[\frac{ik}{\sqrt{1-t^2}} c_{n,k} P_n^k(t) e^{ik\phi} \varepsilon^t - \sqrt{1-t^2} c_{n,k} P_n^{k'}(t) e^{ik\phi} \varepsilon^\phi \right],$$

for $n = 1, \ldots, N; k = 0, \ldots, N$. Thereby, $P_n^{k'}(t)$ denotes the first derivative of $P_n^k(t)$ with respect to t, respectively later on $P_n^{k''}(t)$ the second derivative. Usually, the coefficients $c_{n,k}$ are chosen such that the spherical harmonics are orthonormal with respect to $\langle \cdot, \cdot \rangle_{L^2(\Omega)}$, see, for example, [8]. The negative orders can be obtained by

$$y_{n,-k}^{(3)}(t,\phi) = (-1)^k \left(y_{n,k}^{(3)}(t,\phi) \right)^*, \quad k = 1, \ldots, N.$$

Before entering details of our extended pseudo spectral method, we should outline that the occurring singularities at the poles are of removable type [8]. Moreover, we do not expect computational problems, since we use in latitudinal direction an open Gauss-Legendre quadrature (i.e., the poles do not belong to our integration nodes). The latter fact allows us to handle the terms belonging to ε^ϕ, respectively, ε^t separately. Since both do not depend on the summations, the problem of reconstructing $u_N^{(3)}$ on the same tensor product grid as introduced above, separates outsides the poles into two subproblems, such that

$$u_N^{(3)} = {}^{\varepsilon^t} u^{(3)} \varepsilon^t + {}^{\varepsilon^\phi} u^{(3)} \varepsilon^\phi.$$

Further, we introduce a vectorial expansion and a corresponding scalar reduction between backward and forward transform. Then, the *fast pseudo spectral algorithm* for type 3 vector fields works as follows:

Pseudo Spectral Algorithm for Type 3 Vector Fields: Pseudo spectral transforms are essentially based on the *triangular truncation* notation provided by (5.7) by interchanging the summation for n and k. Moreover, we set $y_{0,0}^{(3)} = 0$ and its "Fourier coefficient" $u_{0,0}^{(3)} = 0$ to benefit in a clear algorithmic structure. This introduced *dummy function* saves us the analogy to the scalar pseudo spectral algorithm (see, for example, [6]). To evaluate $u_N^{(3)} = {}^{\varepsilon^t} u^{(3)} \varepsilon^t + {}^{\varepsilon^\phi} u^{(3)} \varepsilon^\phi$ on the Gauss-Legendre grid [6], we have to compute the quantities

$$
{}^{\varepsilon^t} u_{*,k}^{(3)}(t_j) = \sum_{n=\max\{|k|,1\}}^{N} u_{n,k}^{(3)} \frac{(-1)^k}{\sqrt{n(n+1)}} \frac{ik}{\sqrt{1-t_j^2}} c_{n,k} P_n^k(t_j),
$$

$j = 1, \ldots, N+1; k = 0, \ldots, N$, and

$$\varepsilon^\phi u_{*,k}^{(3)}(t_j) = \sum_{n=\max\{|k|,1\}}^{N} u_{n,k}^{(3)} \frac{-(-1)^k}{\sqrt{n(n+1)}} \sqrt{1-t_j^2} c_{n,k} P_n^{k'}(t_j),$$

$j = 1, \ldots, N+1; k = 0, \ldots, N$.

Since $u_N^{(3)}$ is real, we store $\varepsilon^t u_{*,k}^{(3)}(t_j) = \left(\varepsilon^t u_{*,k}^{(3)}(t_j) \right)^*$ in decreasing order $k = N, \ldots, 1$ column-wise. To evaluate finally $\varepsilon^t u^{(3)}$ on the Gauss-Legendre grid, we apply an inverse FFT in longitudinal direction (row-wise), and expand by ε^t. The same procedure for $\varepsilon^\phi u_{*,k}^{(3)}$, which is associated with ε^ϕ, allows us to reconstruct $u_N^{(3)}(t_j, \phi_i) = \varepsilon^t u^{(3)}(t_j, \phi_i)\varepsilon^t + \varepsilon^\phi u^{(3)}(t_j, \phi_i)\varepsilon^\phi, j = 1, \ldots, N+1; i = 1, \ldots, 2N+1.$

Vice versa, we can determine the Fourier coefficients of $u_N^{(3)}$ by integration: Assume $u_N^{(3)}$ to be real valued in $\mathrm{harm}_{1,\ldots,N}^{(3)}(\Omega)$ to be given on the grid introduced above. By applying Fubini's Theorem, we are able to deduce for the Fourier coefficients $u_{n,k}^{(3)}$ that

$$u_{n,k}^{(3)} = \int_\Omega u^{(3)}(\eta) \cdot y_{n,k}^{(3)*}(\eta) \, dS(\eta) \tag{5.8}$$

$$= \int_{-1}^{1} \Big[\underbrace{\frac{1}{2\pi} \int_0^{2\pi} \left(u^{(3)}(t,\phi) \cdot \varepsilon^t \right) e^{-ik\phi} d\phi}_{= \varepsilon^t u_{*,k}^{(3)}(t)} \Big] \frac{(-1)^k}{\sqrt{n(n+1)}} \frac{-ik}{\sqrt{1-t^2}} c_{n,k} P_n^k(t) dt$$

$$+ \int_{-1}^{1} \Big[\underbrace{\frac{1}{2\pi} \int_0^{2\pi} \left(u^{(3)}(t,\phi) \cdot \varepsilon^\phi \right) e^{-ik\phi} d\phi}_{= \varepsilon^\phi u_{*,k}^{(3)}(t)} \Big] \frac{-(-1)^k}{\sqrt{n(n+1)}} \sqrt{1-t^2} c_{n,k} P_n^{k'}(t) dt$$

$$= \int_{-1}^{1} \varepsilon^t u_{*,k}^{(3)}(t) \frac{(-1)^k}{\sqrt{n(n+1)}} \frac{-ik}{\sqrt{1-t^2}} c_{n,k} P_n^k(t) dt$$

$$+ \int_{-1}^{1} \varepsilon^\phi u_{*,k}^{(3)}(t) \frac{-(-1)^k}{\sqrt{n(n+1)}} \sqrt{1-t^2} c_{n,k} P_n^{k'}(t) dt.$$

Thus, we can apply an FFT in longitudinal direction to evaluate $\varepsilon^t u_{*,k}^{(3)}(t_j), j = 1, \ldots, N+1$, and $\varepsilon^\phi u_{*,k}^{(3)}(t_j), j = 1, \ldots, N+1$, and an exact integration to evaluate for $n = 1, \ldots, N; k = 0, \ldots, N$

$$\varepsilon^t u_{n,k}^{(3)} = \sum_{j=1}^{N+1} w_j \, \varepsilon^t u_{*,k}^{(3)}(t_j) \frac{(-1)^k}{\sqrt{n(n+1)}} \frac{-ik}{\sqrt{1-t_j^2}} c_{n,k} P_n^k(t_j) \tag{5.9}$$

and

$$\varepsilon^\phi u_{n,k}^{(3)} = \sum_{j=1}^{N+1} w_j \, \varepsilon^\phi u_{*,k}^{(3)}(t_j) \frac{-(-1)^k}{\sqrt{n(n+1)}} \sqrt{1-t_j^2} c_{n,k} P_n^{k'}(t_j)$$

such that

$$u_{n,k}^{(3)} = \varepsilon^t u_{n,k}^{(3)} + \varepsilon^\phi u_{n,k}^{(3)}.$$

Since $u_N^{(3)}$ is real, $u_{n,-k}^{(3)}$ is given by

$$u_{n,-k}^{(3)} = (-1)^k u_{n,k}^{(3)*}, \quad k = 1, \ldots, N.$$

The same strategy can be performed analogously for tensor fields (see [10]). The idea for a fast evaluation of the nonlinear advection is to reconstruct $\nabla^* \otimes u$ and u on the exact integration grid and then to compute in the space domain $(\nabla^* \otimes u)^T u$. Consequently, we transform into the Fourier domain to obtain the corresponding coefficients. In addition, it should be remarked that this method also allows the exact separation of vector fields of mixed types, since we apply a polynomially exact integration. The latter is of special importance for the advection.

Before entering into the details of our algorithm we introduce the following abbreviations: For $n = 1, \ldots, N; k = 0, \ldots, N$ we define

$$\varepsilon^t d_{n,k}^{(3)}(t) = \frac{(-1)^k}{\sqrt{n(n+1)}} \frac{ik}{\sqrt{1-t^2}} c_{n,k} P_n^k(t), \tag{5.10}$$

$$\varepsilon^\phi d_{n,k}^{(3)}(t) = -\frac{(-1)^k}{\sqrt{n(n+1)}} \sqrt{1-t^2} c_{n,k} P_n^{k'}(t), \tag{5.11}$$

where the upper left index reflects the association of these terms to ε^t, resp. ε^ϕ. For structural simplicity we let $\varepsilon^t d_{0,0}^{(3)}(t) = 0$ and $\varepsilon^\phi d_{0,0}^{(3)}(t) = 0$ corresponding to the "Fourier coefficient" $u_{0,0}^{(3)} = 0$ operating in the following as a *dummy element*. From the above explained idea, it is advisable to have a closer look to the reconstruction of $\nabla^* \otimes u^{(3)} = \mathbf{u}^{(2,3)}$ tensor fields. These tensor fields can be written as

$$\mathbf{u}^{(2,3)}(\eta) = \sum_{n=1}^N \sum_{k=-n}^n u_{n,k}^{(2,3)} (\nabla_\eta^* \otimes y_{n,k}^{(3)})(\eta)$$

$$= \sum_{k=-N}^N \sum_{n=\max\{|k|,1\}}^N u_{n,k}^{(2,3)} (\nabla_\eta^* \otimes y_{n,k}^{(3)})(\eta).$$

From (2.1) we have $\mathbf{y}_{n,k}^{(2,3)}(\eta) = (\nabla_\eta^* \otimes y_{n,k}^{(3)})(\eta)$. By some minor calculation we derive a representation of $\mathbf{y}_{n,k}^{(2,3)}$ that allow us again to separate scalar latitudinal and

longitudinal terms:

$$\mathbf{y}_{n,k}^{(2,3)}(t,\phi) = e^{ik\phi}\Bigg\{ \tag{5.12}$$

$$\left[\frac{-ik(-1)^k}{\sqrt{n(n+1)}}c_{n,k}P_n^{k'}(t) - \frac{t}{1-t^2}\frac{ik}{\sqrt{n(n+1)}}(-1)^k c_{n,k}P_n^k(t)\right]\varepsilon^\phi \otimes \varepsilon^\phi$$

$$+ \left[\frac{-k^2}{1-t^2}\frac{1}{\sqrt{n(n+1)}}(-1)^k c_{n,k}P_n^k(t)\right]\varepsilon^\phi \otimes \varepsilon^t$$

$$+ \left[\frac{t}{\sqrt{n(n+1)}}(-1)^k c_{n,k}P_n^{k'}(t) - \frac{1-t^2}{\sqrt{n(n+1)}}(-1)^k c_{n,k}P_n^{k''}(t)\right]\varepsilon^t \otimes \varepsilon^\phi$$

$$+ \left[\frac{ik}{\sqrt{n(n+1)}}(-1)^k c_{n,k}P_n^k(t)\right]\varepsilon^t \otimes \frac{\partial}{\partial t}\varepsilon^t$$

$$+ \left[\frac{-1}{\sqrt{n(n+1)}}(-1)^k c_{n,k}P_n^{k'}(t)\right]\varepsilon^\phi \otimes \frac{\partial}{\partial \phi}\varepsilon^\phi$$

$$+ \left[\frac{t}{1-t^2}\frac{ik}{\sqrt{n(n+1)}}(-1)^k c_{n,k}P_n^k(t) + \frac{ik}{\sqrt{n(n+1)}}(-1)^k c_{n,k}P_n^{k'}(t)\right]\varepsilon^t \otimes \varepsilon^t\Bigg\},$$

for $n = 1, \ldots, N; k = 0, \ldots, N$. The negative orders can be obtained by observing

$$\mathbf{y}_{n,-k}^{(2,3)} = (-1)^k \left(\mathbf{y}_{n,k}^{(2,3)}\right)^*.$$

It turns out that the problem of reconstructing $\mathbf{u}^{(2,3)}$ on the same tensor product grid as introduced above, separates into six subproblems, namely

$$\mathbf{u}^{(2,3)} = {}^{\varepsilon^\phi \otimes \varepsilon^\phi}u^{(2,3)}\varepsilon^\phi \otimes \varepsilon^\phi + {}^{\varepsilon^\phi \otimes \varepsilon^t}u^{(2,3)}\varepsilon^\phi \otimes \varepsilon^t + {}^{\varepsilon^t \otimes \varepsilon^\phi}u^{(2,3)}\varepsilon^t \otimes \varepsilon^\phi$$

$$+ {}^{\varepsilon^t \otimes \frac{\partial}{\partial t}\varepsilon^t}u^{(2,3)}\varepsilon^t \otimes \frac{\partial}{\partial t}\varepsilon^t + {}^{\varepsilon^\phi \otimes \frac{\partial}{\partial \phi}\varepsilon^\phi}u^{(2,3)}\varepsilon^\phi \otimes \frac{\partial}{\partial \phi}\varepsilon^\phi + {}^{\varepsilon^t \otimes \varepsilon^t}u^{(2,3)}\varepsilon^t \otimes \varepsilon^t.$$

According to this partition we introduce the following six functions (in analogy to the *reduced matrix elements* known from quantum mechanics [5]) by

$${}^{\varepsilon^\phi \otimes \varepsilon^\phi}d_{n,k}^{(2,3)}(t) = \frac{-ik(-1)^k}{\sqrt{n(n+1)}}c_{n,k}P_n^{k'}(t) - \frac{t}{1-t^2}\frac{ik}{\sqrt{n(n+1)}}(-1)^k c_{n,k}P_n^k(t), \tag{5.13}$$

$${}^{\varepsilon^\phi \otimes \varepsilon^t}d_{n,k}^{(2,3)}(t) = \frac{-k^2}{1-t^2}\frac{1}{\sqrt{n(n+1)}}(-1)^k c_{n,k}P_n^k(t),$$

$${}^{\varepsilon^t \otimes \varepsilon^\phi}d_{n,k}^{(2,3)}(t) = \frac{t}{\sqrt{n(n+1)}}(-1)^k c_{n,k}P_n^{k'}(t) - \frac{1-t^2}{\sqrt{n(n+1)}}(-1)^k c_{n,k}P_n^{k''}(t),$$

$${}^{\varepsilon^t \otimes \frac{\partial}{\partial t}\varepsilon^t}d_{n,k}^{(2,3)}(t) = \frac{ik}{\sqrt{n(n+1)}}(-1)^k c_{n,k}P_n^k(t),$$

$${}^{\varepsilon^\phi \otimes \frac{\partial}{\partial \phi}\varepsilon^\phi}d_{n,k}^{(2,3)}(t) = \frac{-1}{\sqrt{n(n+1)}}(-1)^k c_{n,k}P_n^{k'}(t),$$

$${}^{\varepsilon^t \otimes \varepsilon^t}d_{n,k}^{(2,3)}(t) = \frac{t}{1-t^2}\frac{ik}{\sqrt{n(n+1)}}(-1)^k c_{n,k}P_n^k(t) + \frac{ik}{\sqrt{n(n+1)}}(-1)^k c_{n,k}P_n^{k'}(t),$$

for $n = 1, \ldots, N; k = 0, \ldots, N$.

Note that the upper left index reflects the association of these terms to the corresponding tensors.

To save us a clear matrix-vector notation, we again introduce dummy elements, viz.

$$\varepsilon^\phi \otimes \varepsilon^\phi d_{0,0}^{(2,3)}(t) = 0, \qquad \varepsilon^\phi \otimes \varepsilon^t d_{0,0}^{(2,3)}(t) = 0,$$

$$\varepsilon^t \otimes \varepsilon^\phi d_{0,0}^{(2,3)}(t) = 0, \qquad \varepsilon^t \otimes \frac{\partial}{\partial t} \varepsilon^t d_{0,0}^{(2,3)}(t) = 0,$$

$$\varepsilon^\phi \otimes \frac{\partial}{\partial \phi} \varepsilon^\phi d_{0,0}^{(2,3)}(t) = 0, \qquad \varepsilon^t \otimes \varepsilon^t d_{0,0}^{(2,3)}(t) = 0,$$

$$u_{0,0}^{(2,3)} = 0.$$

Then, except for the vectorial expansion, the backward transform into the space domain works in analogy to the type 3 vector spherical harmonic case. Accordingly, the vectorial expansion is substituted by the corresponding tensorial expansion.

ALGORITHM 5.5 (FSPM for the Nonlinear Advection Term).

Purpose: *The algorithm computes the Fourier coefficients* $v_{n,k}^{(3)}$ *corresponding to* $v = (u \cdot \nabla^*)u = (\nabla^* \otimes u)^T u$. *In the first part of this algorithm we evaluate the tensorial term* $[(\nabla_\eta^* \otimes u)(\eta)]^T$, *and then the vectorial term* $u(\eta)$ *of the integrand.*

We use in the following the Gauss-Legendre integration grid: The grid points (t_j, ϕ_i) *are given by* $\phi_i = 2\pi(i-1)/(4N+1), i = 1, \ldots, 4N+1$, *and* $t_j, j = 1, \ldots, 2N+1$, *where the latter denote the Gauss-Legendre integration nodes with corresponding weights* $w_j, j = 1, \ldots, 2N+1$. *This grid yields a cubature rule which allows polynomial exact integration up to degree* $2(2N+1) - 1 = 4N+1$.

1. **Evaluate $(\nabla^* \otimes u)$ in the Space Domain:**

(i) *Compute the quantities* $\varepsilon^\phi \otimes \varepsilon^\phi u_{*,k}^{(2,3)}(t_j) = \sum_{n=|k|}^{N} u_{n,k}^{(3)} \varepsilon^\phi \otimes \varepsilon^\phi d_{n,k}^{(2,3)}(t_j)$, *for* $k = 0, \ldots, N; j = 1, \ldots, 2N+1$. *This can be achieved by applying an inverse Gauss-Legendre Transformation (GLT). Assume that the $N+1$ (rectangular) Gauss-Legendre matrices have been tabulated beforehand. Equipped with them, perform matrix-vector products between*

$$\varepsilon^\phi \otimes \varepsilon^\phi D_k^{(2,3)} = \begin{pmatrix} \varepsilon^\phi \otimes \varepsilon^\phi d_{k,k}^{(2,3)}(t_1) & \varepsilon^\phi \otimes \varepsilon^\phi d_{k+1,k}^{(2,3)}(t_1) & \cdots & \varepsilon^\phi \otimes \varepsilon^\phi d_{N,k}^{(2,3)}(t_1) \\ \varepsilon^\phi \otimes \varepsilon^\phi d_{k,k}^{(2,3)}(t_2) & \varepsilon^\phi \otimes \varepsilon^\phi d_{k+1,k}^{(2,3)}(t_2) & \cdots & \varepsilon^\phi \otimes \varepsilon^\phi d_{N,k}^{(2,3)}(t_2) \\ \vdots & \vdots & & \vdots \\ \varepsilon^\phi \otimes \varepsilon^\phi d_{k,k}^{(2,3)}(t_{2N+1}) & \varepsilon^\phi \otimes \varepsilon^\phi d_{k+1,k}^{(2,3)}(t_{2N+1}) & \cdots & \varepsilon^\phi \otimes \varepsilon^\phi d_{N,k}^{(2,3)}(t_{2N+1}) \end{pmatrix}$$

$$and \qquad u_{*,k} = \begin{pmatrix} u_{k,k}^{(3)} & u_{k+1,k}^{(3)} & \cdots & u_{N,k}^{(3)} \end{pmatrix}^T \tag{5.14}$$

to obtain the vectors

$$\varepsilon^\phi \otimes \varepsilon^\phi D_k^{(2,3)} u_{*,k} = \varepsilon^\phi \otimes \varepsilon^\phi u_{*,k}^{(2,3)}, \tag{5.15}$$

for $k = 0, \ldots, N$. *Assume that the column vectors* $\varepsilon^\phi \otimes \varepsilon^\phi u_{*,k}^{(2,3)}, k = 0, \ldots, N$ *are stored in the first $N+1$ columns of a $(2N+1) \times (4N+1)$ matrix. Compute* $\varepsilon^\phi \otimes \varepsilon^\phi u_{*,k}^{(2,3)}$ *for*

the negative orders by

$$\varepsilon^\phi \otimes \varepsilon^\phi u_{*,-k}^{(2,3)}(t_j) = \left(\varepsilon^\phi \otimes \varepsilon^\phi u_{*,k}^{(2,3)}(t_j), \right)^* \quad k = 1, \dots, N; j = 1, \dots, 2N + 1.$$

Then, store these vectors in descending order in the columns of this matrix starting from the most right with order -1. The remaining columns are filled up with zeros:

$$\left(\begin{array}{ccccccccc} \varepsilon^\phi \otimes \varepsilon^\phi u_{*,0}^{(2,3)} & \dots & \varepsilon^\phi \otimes \varepsilon^\phi u_{*,N}^{(2,3)} & 0 & \dots & 0 & \varepsilon^\phi \otimes \varepsilon^\phi u_{*,-N}^{(2,3)} & \dots & \varepsilon^\phi \otimes \varepsilon^\phi u_{*,-1}^{(2,3)} \end{array} \right)$$

(ii) *Apply row-wise an inverse FFT and obtain immediately the grid values* $\varepsilon^\phi \otimes \varepsilon^\phi u^{(2,3)}(t_j, \phi_i), j = 1, \dots, 2N + 1; i = 1, \dots, 4N + 1.$

2. *Repeat the last step analogously for*

$$\varepsilon^\phi \otimes \varepsilon^t d_{n,k}^{(2,3)}, \quad \varepsilon^t \otimes \varepsilon^\phi d_{n,k}^{(2,3)}, \quad \varepsilon^t \otimes \frac{\partial}{\partial t} \varepsilon^t d_{n,k}^{(2,3)}, \quad \varepsilon^\phi \otimes \frac{\partial}{\partial \phi} \varepsilon^\phi d_{n,k}^{(2,3)}, \quad \varepsilon^t \otimes \varepsilon^t d_{n,k}^{(2,3)},$$

to obtain the quantities $\varepsilon^\phi \otimes \varepsilon^t u^{(2,3)}$, $\varepsilon^t \otimes \varepsilon^\phi u^{(2,3)}$, $\varepsilon^t \otimes \frac{\partial}{\partial t} \varepsilon^t u^{(2,3)}$, $\varepsilon^\phi \otimes \frac{\partial}{\partial \phi} \varepsilon^\phi u^{(2,3)}$ *and* $\varepsilon^t \otimes \varepsilon^t u^{(2,3)}$ *evaluated on the grid* $\{t_j, \phi_i\}, j = 1, \dots, 2N + 1; i = 1, \dots, 4N + 1.$

3. ***Tensorial Expansion:***
Compute the desired tensor on the grid by

$$\mathbf{u}^{(2,3)}(t_j, \phi_i) = [\, \varepsilon^\phi \otimes \varepsilon^\phi u^{(2,3)} \varepsilon^\phi \otimes \varepsilon^\phi](t_j, \phi_i) + [\, \varepsilon^\phi \otimes \varepsilon^t u^{(2,3)} \varepsilon^\phi \otimes \varepsilon^t](t_j, \phi_i)$$

$$+ [\, \varepsilon^t \otimes \varepsilon^\phi u^{(2,3)} \varepsilon^t \otimes \varepsilon^\phi](t_j, \phi_i) + [\, \varepsilon^t \otimes \frac{\partial}{\partial t} \varepsilon^t u^{(2,3)} \varepsilon^t \otimes \varepsilon^{\frac{\partial}{\partial t}}]$$

$$+ [\, \varepsilon^\phi \otimes \frac{\partial}{\partial \phi} \varepsilon^\phi u^{(2,3)} \varepsilon^\phi \otimes \frac{\partial}{\partial \phi} \varepsilon^\phi](t_j, \phi_i) + [\, \varepsilon^t \otimes \varepsilon^t u^{(2,3)} \varepsilon^t \otimes \varepsilon^t](t_j, \phi_i),$$

for $j = 1, \dots, 2N + 1; i = 1, \dots, 4N + 1.$

4. ***Evaluate u in the Space Domain:***
(i) *Compute the quantities* $\varepsilon^t u_{*,k}^{(3)}(t_j) = \sum_{n=|k|}^{N} u_{n,k} \varepsilon^t d_{n,k}^{(3)}(t_j)$, *for $k = 0, \dots, N$; $j = 1, \dots, 2N + 1$. This can be achieved by applying an inverse Gauss-Legendre Transformation (GLT). Assume that the $N + 1$ (rectangular) Gauss-Legendre matrices have been tabulated beforehand. Analogously to (5.15) we perform matrix-vector products between*

$$\varepsilon^t D_k^{(3)} = \begin{pmatrix} \varepsilon^t d_{k,k}^{(3)}(t_1) & \varepsilon^t d_{k+1,k}^{(3)}(t_1) & \dots & \varepsilon^t d_{N,k}^{(3)}(t_1) \\ \varepsilon^t d_{k,k}^{(3)}(t_2) & \varepsilon^t d_{k+1,k}^{(3)}(t_2) & \dots & \varepsilon^t d_{N,k}^{(3)}(t_2) \\ \vdots & \vdots & & \vdots \\ \varepsilon^t d_{k,k}^{(3)}(t_{2N+1}) & \varepsilon^t d_{k+1,k}^{(3)}(t_{2N+1}) & \dots & \varepsilon^t d_{N,k}^{(3)}(t_{2N+1}) \end{pmatrix}$$

and $u_{*,k}$ from (5.14) to obtain the vectors

$$\varepsilon^t D_k^{(3)} u_{*,k} = \varepsilon^t u_{*,k}^{(3)}, \tag{5.16}$$

for $k = 0, \dots, N$. Assume that the column vectors $\varepsilon^t u_{*,k}^{(3)}, k = 0, \dots, N$ are stored in the first $N + 1$ columns of a $(2N + 1) \times (4N + 1)$ matrix. Compute $\varepsilon^t u_{*,k}^{(3)}$ for the negative orders by

$$\varepsilon^t u_{*,-k}^{(3)}(t_j) = \left(\varepsilon^t u_{*,k}^{(3)}(t_j) \right)^*, \quad k = 1, \dots, N; j = 1, \dots, 2N + 1.$$

Then, store these vectors in descending order in the columns of this matrix starting from the most right with order -1. The remaining columns are filled up with zeros:

$$\left(\begin{array}{ccccccccc} \varepsilon^t u_{*,0}^{(3)} & \dots & \varepsilon^t u_{*,N}^{(3)} & 0 & \dots & 0 & \varepsilon^t u_{*,-N}^{(3)} & \dots & \varepsilon^t u_{*,-1}^{(3)} \end{array} \right)$$

(ii) *Apply row-wise an inverse FFT and obtain immediately the grid values* $\varepsilon^t u^{(3)}(t_j, \phi_i), j = 1, \ldots, 2N+1; i = 1, \ldots, 4N+1.$

5. *Repeat the last step analogously for* $\varepsilon^\phi d_{n,k}^{(3)}(t)$ *to obtain the quantities* $\varepsilon^\phi u^{(3)}(t_j, \phi_i)$ *evaluated on the grid* $\{(t_j, \phi_i)\}, j = 1, \ldots, 2N+1; i = 1, \ldots, 4N+1.$

6. **Vectorial Expansion:**
Compute the desired vector field on the grid by

$$u(t_j, \phi_i) = [\,\varepsilon^t u^{(3)} \varepsilon^t](t_j, \phi_i) + [\,\varepsilon^\phi u^{(3)} \varepsilon^\phi](t_j, \phi_i)$$

for $j = 1, \ldots, 2N+1; i = 1, \ldots, 4N+1.$

7. **Compute the Integrand** $(\nabla \otimes u)^T u$ **in the Space Domain:**
Compute on the grid the vector field v:

$$v(t_j, \phi_i) = [(\mathbf{u}^{(2,3)})^T u](t_j, \phi_i), j = 1, \ldots, 2N+1; i = 1, \ldots, 4N+1.$$

8. **Scalar Reduction:**
Form the inner product with $\varepsilon^t(t_j, \phi_i), j = 1, \ldots, N+1; i = 1, \ldots, 2N+1$, which projects the vector field on its $\varepsilon^t v$ content. Analogously, we obtain the projection on its $\varepsilon^\phi v$ content. It should be remarked that v is a vector field of mixed type, namely of type 2 and type 3. By using implicitly a polynomial exact integration against $y_{n,k}^{(3)}$ we are able to separate the desired type 3 part.

9. **Recovery of the Fourier Coefficients:**
To transform into the Fourier Domain, we apply row-wise a forward FFTs to determine the quantities $\varepsilon^t v_{*,k}(t_j), j = 1, \ldots, 2N+1; k = 0, \ldots, 2N$. This corresponds to the first $2N+1$ column vectors $\varepsilon^t v_{*,k}$.

We conclude the algorithm by applying the forward GLT by computing the $2N+1$ matrix-vector products between

$$\varepsilon^t \widetilde{D}_k^{(3)} = \frac{2\pi}{4N+1} \begin{pmatrix} w_1\,\varepsilon^t d_{k,k}^{(3)}(t_1) & w_2\,\varepsilon^t d_{k,k}^{(3)}(t_2) & \ldots & w_n\,\varepsilon^t d_{k,k}^{(3)}(t_{2N+1}) \\ w_1\,\varepsilon^t d_{k+1,k}^{(3)}(t_1) & w_2\,\varepsilon^t d_{k+1,k}^{(3)}(t_2) & \ldots & w_n\,\varepsilon^t d_{k+1,k}^{(3)}(t_{2N+1}) \\ \vdots & \vdots & & \vdots \\ w_1\,\varepsilon^t d_{2N,k}^{(3)}(t_1) & w_2\,\varepsilon^t d_{2N,k}^{(3)}(t_2) & \ldots & w_n\,\varepsilon^t d_{2N,k}^{(3)}(t_{2N+1}) \end{pmatrix}$$

and $\varepsilon^t v_{*,k}$ to obtain the the Fourier coefficients corresponding to ε^t

$$\varepsilon^t \widetilde{D}_k^{(3)} \begin{pmatrix} \varepsilon^t v_{*,k}(t_1) \\ \varepsilon^t v_{*,k}(t_2) \\ \vdots \\ \varepsilon^t v_{*,k}(t_{2N+1}) \end{pmatrix} = \begin{pmatrix} \varepsilon^t v_{k,k} \\ \varepsilon^t v_{k+1,k} \\ \vdots \\ \varepsilon^t v_{2N,k} \end{pmatrix}, \tag{5.17}$$

for $k = 0, \ldots, 2N$. Analogously, we find $\varepsilon^\phi v_{n,k}, n = 0, \ldots, 2N; k = 0, \ldots, n$, such that we get finally the type 3 Fourier coefficients of v by

$$v_{n,k}^{(3)} = \varepsilon^t v_{n,k} + \varepsilon^\phi v_{n,k}, \qquad n = 0, \ldots, 2N; k = 0, \ldots, n,$$

and with

$$v_{n,-k}^{(3)} = (-1)^k \left(v_{n,k}^{(3)}\right)^*, \qquad k = 1, \ldots, n,$$

the negative orders, since v is real.

Algorithmic effort: We have to perform 6 GLTs to reconstruct the tensor on the grid and 2 GLTs for the velocity field u. Beyond that, we have for the transform back into the Fourier domain 2 additional GLTs, which yields finally for the storage of the a priori calculated GLT matrices

$$(6+2)\sum_{k=0}^{N}(2N+1)(N-k+1)+2\sum_{k=0}^{2N}(2N+1)(2N-k+1)\approx 16N^3. \qquad (5.18)$$

The algorithmic effort scales analogously with $O(N^3)$. Namely, the $N+1$, resp. $2N+1$ matrix-vector products in (5.15), (5.16) and (5.17) cost

$$(6+2)\sum_{k=0}^{N}(2N+1)(N-k+1)+2\sum_{k=0}^{2N}(2N+1)(2N-k+1)\approx 16N^3$$

real×complex multiplications, each of which is equivalent to 2 real multiplications. Additionally, we have twice as much complex-complex additions, which are equivalent to two real additions. Thus, the GLT leads us to about $32N^3$ real multiplications, and about $64N^3$ real additions. In between, the complex FFTs (not necessarily complex, one could also use complex-to-real and real-to-complex FFTs) requires each about $8N\log_2 N$ real multiplications, and $12N\log_2 N$ real additions. Thus all FFTs require $(6+2+2)(2N+1)8N\log_2 N \approx 160N^2\log_2 N$ multiplications and $(6+2+2)(2N+1)12N\log_2 N \approx 240N^2\log_2 N$ additions. Keeping in mind that we have $\approx 8N^2$ grid points, the vectorial and tensorial expansion, the remaining matrix-vector product in the space domain, and then, the scalar reduction, see step 8. in Algorithm 5.5, requires approximately

$$8N^2(6\cdot 9+2\cdot 3+9+2\cdot 3)\approx 600N^2$$

complex×complex multiplications, which is equivalent to $2400N^2$ real multiplications and $1200N^2$ real additions. Obviously, the algorithm profits from the semi-linear scaling of the FFTs. Thus, the whole procedure is dominated by the GLT and scales with $O(N^3)$ while the break even point is approximately at $N=12$. Since we use in our simulations (also with respect to applications in meteorology) much larger basis sets, we obtain, for example, at $N=100$ a speedup factor of 500!

6. Numerical Results. In this section we report numerical results obtained by using the nonlinear Galerkin method. To demonstrate the efficiency of our method, we study an example, that is motivated by [7] for a toroidal domain, i.e., the two-dimensional periodic case. However, we study here an extension of [7] to the rotating sphere by involving a Coriolis term and, moreover, time-dependent flow driving forces. Finally, we compare the nonlinear Galerkin method with the linear one, which can be obtained by setting $z_m=0$.

Description of the Computations: The initial condition $u_0 = u_0/\|u_0\|_{l^\Omega}$, with $u_0 = \sum_{n=1}^{20}\sum_{k=-n}^{n} u_{n,k}^{(3)} y_{n,k}^{(3)}$ is computed from a given spectrum given by

$$u_{n,k}^{(3)} = \frac{2}{n+(\sqrt{\nu}n)^5}e^{i\theta_k}, \qquad \text{for} \quad n=1,\dots,20; k=0,\dots,n$$

where $\theta_0 = 0$, and $\theta_k, k=1,\dots,n$ is generated by a random function. The negative orders are obtained by $u_{n,-k} = (-1)^k u_{n,k}^*$. The viscosity ν is set to $\nu = 10^{-4}$. This

example is chosen in analogy to [7]. Obviously, the initial spectrum decays like n^{-1}. As Fig. 6.1 shows the flow has no organized structures and visible vortices. Moreover, the flow is driven by some time-dependent (decaying), external force f, given by

$$f(t,\eta) = \gamma(t)y^{(3)}_{3,0}(\eta), \qquad \eta \in \Omega,$$

with

$$\gamma(t) = \begin{cases} 1 & \text{for } t \in [0,10] \\ \cos(\pi/5t)e^{-(t-10)/5} & \text{for } t \in (10,60]. \end{cases}$$

In order to describe all the scales of motion, the spherical harmonics degree k_N must be chosen so that an associated (spherical grid) size $2\pi/N$ is smaller than the dissipative (Kraichnan) scale l_η; in terms of the spherical harmonic degree it means $k_N > k_\eta$. We recall that under the dissipative scales the motion is damped by viscosity. In fact, the total number of degree of freedom needed to describe the motion, from dissipative scales to large scales containing eddies, can be estimated by the ratio $(k_\eta/k_N)^2$ (see, for example, [7]).
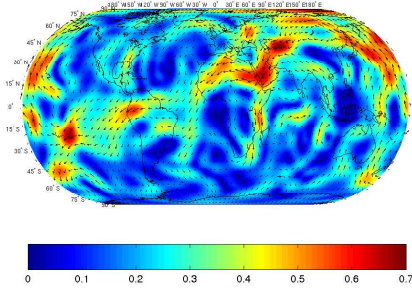
FIG. 6.1. *Initial Flow Velocity at t=0.*
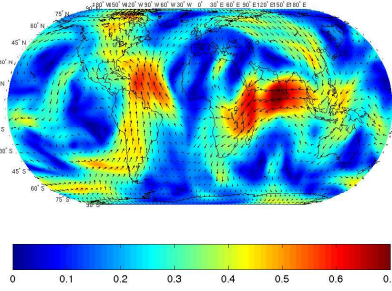
FIG. 6.2. *Flow at t=5.*
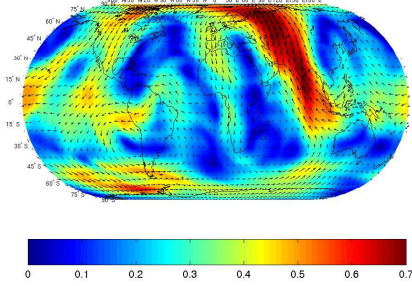
FIG. 6.3. *Flow Velocity at t=10.*
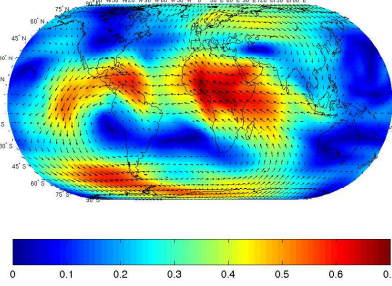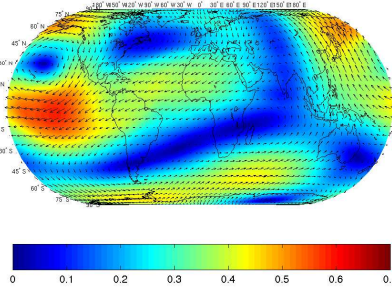

FIG. 6.4. *Flow Velocity at t=20.*
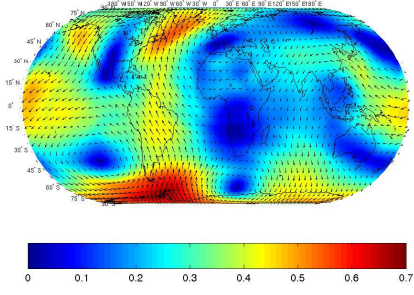
FIG. 6.5. *Flow Velocity at t=30.*
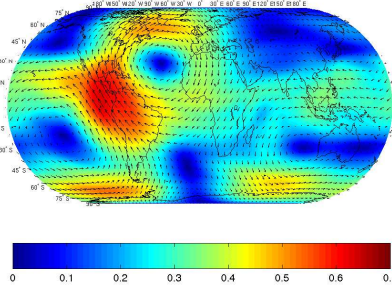
FIG. 6.6. *Flow Velocity at t=40.*
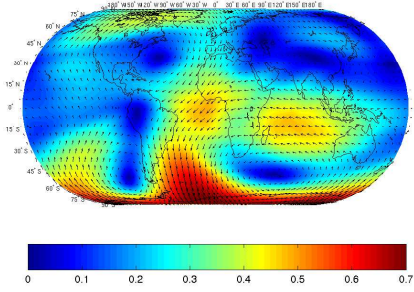
FIG. 6.7. *Flow Velocity at t=50.*

FIG. 6.8. *Flow Velocity at t=60.*

This quantity is related to the dimension of the attractor of the Navier-Stokes equations

$$\left(\frac{k_\eta}{k_N}\right)^2 \approx \mathrm{Re},$$

where Re is the integral scale Reynolds number. The Reynolds number can be defined by

$$\mathrm{Re} = \frac{LU}{\nu},$$

where U denotes the *characteristic* velocity of the flow, and $L = 1/k_N$ the integral length scale defined by

$$L = \frac{U}{\sqrt{2}\eta^{1/3}},$$

with $\eta = \nu\|\Delta^*u\|^2_{l^2(\Omega)}/|\Omega|$. Then $L \approx 0.7$, and $U \approx 0.3$, so that Re ≈ 2100. The dissipative wave number can be estimated by $k_\eta^2 = \mathrm{Re}\cdot k_N^2$, such that $k_\eta \approx 50$. Finally we take the angular velocity $|\omega| = 2.0$ such that the Rossby number relating the advection and Coriolis term reads as follows

$$R_o = \frac{U}{L|\omega|} \approx 0.2.$$

Obviously, this Rossby number is not much smaller than 1, which indicates that the Coriolis term is in the same order as the advection term. In order to be sure to resolve

all the scales of the considered flow, we set the truncation level to a spherical harmonic degree of 100. According to (4.1) and (4.2) this truncation level corresponds to $m = 50$. In detail, the low-frequent approximation u_{50} is represented by spherical harmonics up to degree 50, whereas the high-frequent approximation z_{50} covers the terms up to degree 100. The results for the flow velocity of our simulation is plotted in Fig. 6.1 - Fig. 6.8.
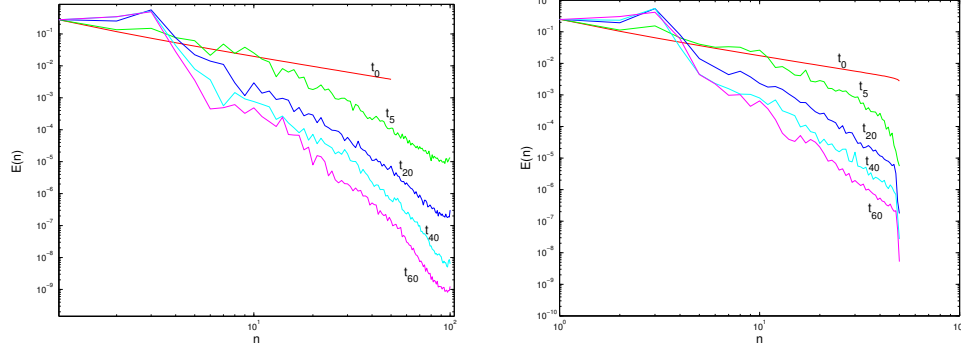

FIG. 6.9. *Comparison of the energy spectrum $E(n)$ for the linear (left) and for the nonlinear (right) Galerkin method with truncation level $N = 100$ at different time steps.*
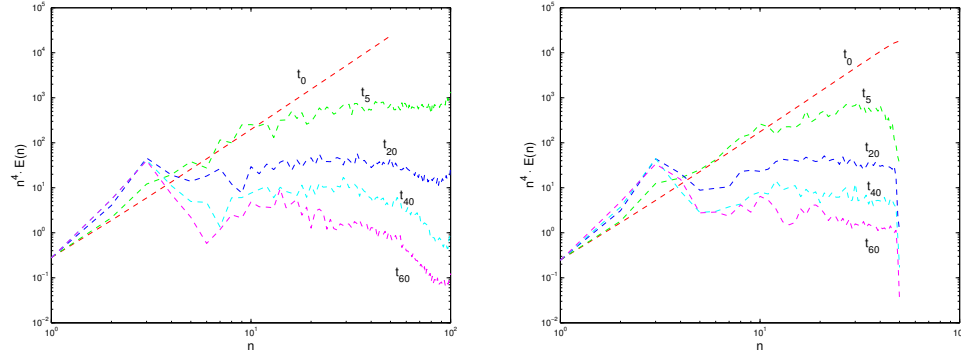
FIG. 6.10. *Comparison of the decay of the energy spectrum $E(n)$ of the linear Galerkin method (left) and the nonlinear Galerkin method (right) with truncation level $N = 100$ at different time steps. We observe a n^{-4}-decay in both energy spectra after some eddy-turnover times.*
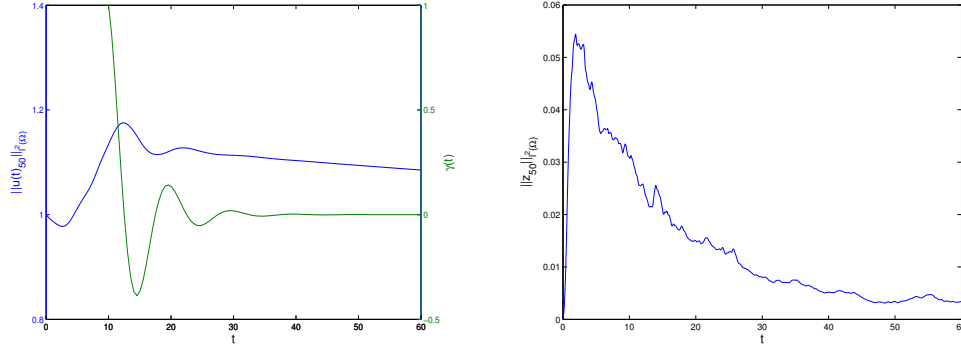

FIG. 6.11. *Time evolution of $\|u_{50}(t)\|_{l^2(\Omega)}$ and $\gamma(t)$ (left), and of $\|z_{50}(t)\|_{l^2(\Omega)}$ (right).*

Now, it appears that the dissipation wave number k_η is of order 42 and varies slightly between 40 and 45 during the computation. Hence, the previous estimate based on the dimension of the attractor matches the computational results. We also remark that if, at $t = 0$, the small scales corresponding to a spherical harmonic degree larger than 20 are set to zero, then a dissipation range appears very quickly, as we can see in Fig. 6.9 at $t = 5$. The enstrophy transfer from the large scales to the small ones acts on the smallest scales after a few iterations. Fig. 6.11 illustrating $\|z_{50}\|_{l^2(\Omega)}$ indicates that this transition period is very short. After this period, the smaller scales are damped by viscosity until an equilibrium between viscous and nonlinear terms appears. Thenceforward, we can see that $\|z_{50}\|_{l^2(\Omega)}$ develops completely independently of $\|u_{50}\|_{l^2(\Omega)}$, see Fig. 6.11. The $l^2(\Omega)$-norm of the Galerkin approximation u_{50} depends also on the forcing term f which varies over time. This dependency is illustrated in Fig. 6.11, which shows also $\gamma(t)$. It is interesting to note, that at $t \approx 30$ the viscous term dominates the external force f, and the energy decays.

As Fig. 6.1 - Fig. 6.8 show the small random structures of the flow at the initial time disappear quickly; fusions of these very small structures lead to larger ones. So, after a transient period, the flow is mainly constituted by large structures.

This can be also studied by looking at the energy spectrum, see Fig. 6.9. The energy spectrum is given by

$$E(n) = \sum_{k=-n}^{n} |u_{n,k}^{(3)}|^2$$

showing the energy contained in each degree averaged overall orders. It is interesting to note, that after a short transient time an initial range is appearing. And we note that more and more energy is transferred into the low-frequent parts of the flow (large eddies). Moreover, let us study the energy decay of the Fourier modes from Fig. 6.10. From this illustration we observe an approximate n^{-4}-decay that has been also reported by Temam [7] for a flow in a two-dimensional, periodic geometry, i.e., on a torus. Evidently, the decay of energy is more rapid than the n^{-3}-decay predicted by Kraichnan's phenomenological theory of turbulence [16]. But our results are in agreement with the ones obtained by Brachet et al. [4] and Orszag [20], who show that a n^{-3}-energy spectrum can only be obtained when the Reynolds number is much larger, e.g., of the order of $2.5 \cdot 10^4$ (see [20]).

The time step is chosen according to accuracy and stability considerations. To ensure the stability, the time step h must satisfy a CFL condition like

$$hN\|u\|_{l^\infty(\Omega)} < 1. \tag{6.1}$$

Having tracked the $l^\infty(\Omega)$-norm of u on a grid, $\|u\|_{l^\infty(\Omega)}$ reached a maximum of 0.72 satisfying (6.1). Since we used a Runge-Kutta solver of forth order for the time-integration, a time-step of 10^{-3} allows most of the spectrum to be recovered. Thus, the global accuracy is then of order 10^{-12}.

With the characteristic length scale L and velocity U, we define a characteristic time unit by the ratio
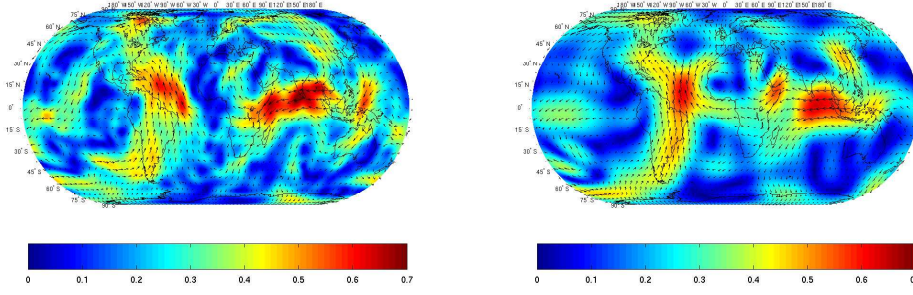
$$\tau = \frac{L}{U},$$

FIG. 6.12. *Comparison of the velocity structures obtained with the linear Galerkin method (left) and the nonlinear Galerkin method (right) at truncation level $N = 30$ and time $t=5$.*
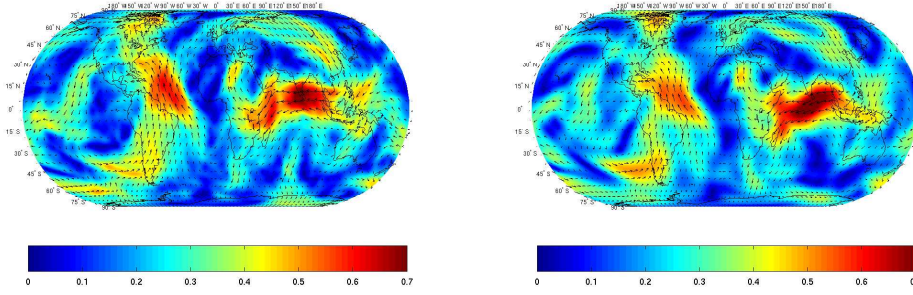

FIG. 6.13. *Comparison of the velocity structures obtained with the linear Galerkin method (left) and the nonlinear Galerkin method (right) at truncation level $N = 50$ and time $t=5$.*
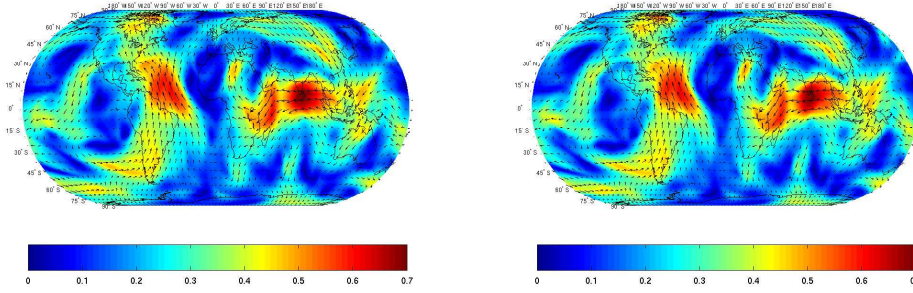

FIG. 6.14. *Comparison of the Velocity Structures obtained with the linear Galerkin method (left) and the nonlinear Galerkin method (right) at truncation level $N = 100$ and time $t=5$.*

which is called eddy-turnover time. This quantity is of order 2.33 for the flow considered. We have let the flow evolve on over $6 \cdot 10^4$ iterations, i.e., on the time interval $[0, 60]$, which correspond to more than 25 time units. The code has been implemented in Fortran 90 using Intel's Fortran Compiler and Math Kernel Library (MKL) to perform the FFTs and BLAS calls. The computation required more than 120 hours of CPU time on a Pentium-4 (3.2 GHz), without counting all the preliminary tests needed to develop and improve the algorithm.

Mesh Refinement and Comparison to the Linear Galerkin Method. The strength of the nonlinear Galerkin method is to represent the considered flow with fewer degrees of freedoms than required by a linear Galerkin scheme. This is observed by obtaining similar results for the same problem in less time. In detail, we compare

at a fixed time $t = 5$ and at different truncation levels $N = \{30, 50, 100\}$ the linear and nonlinear scheme in Fig. 6.12 - 6.14. In case of the linear Galerkin method the *truncation level N* denotes that all scales of motion up to degree N are resolved. The mesh refinement indicates for both schemes that they are stable: In detail, we see in Fig. 6.12 that the linear Galerkin method shows some high-frequent flicker that is induced by higher frequent scales of u_0 that are not resolved. This flicker becomes less for $N = 50$ and disappears when the truncation level is increased to $N = 100$, see Fig. 6.13 and Fig. 6.14. Moreover, it should be outlined that the nonlinear method is about 20% faster than the linear Galerkin method (for the same resolution). Finally, a closer look to the tails of the energy spectrum in Fig. 6.9 and Fig. 6.10 shows a small increase in the Fourier coefficients in case of the linear method. This effect is known as *spectral blocking* and is induced by aliasing effects, see Fig. 6.13 and, for example, Boyd [3]. In Fig. 6.14 we observe a rapid decrease in the tails of the energy spectrum. This effect is inherent to nonlinear Galerkin methods and known as *artificial viscosity* which stabilizes the whole solution procedure (see [3, 7]).

Concluding Remarks. In this work we introduced a nonlinear Galerkin method which is applied to the inhomogenous, incompressible Navier-Stokes equation on the sphere. The arising coupling terms are expressed by Wigner-$3j$ symbols known from quantum mechanics. To increase the efficiency, we extended the idea of FFT-based pseudo spectral algorithms to the rapid evaluation of the considered type 3 vector and tensor fields. This allows us to compute in each time step the coupling integrals of the nonlinear advection term at once yielding finally a $O(N^3)$ method. Finally, we demonstrated the algorithm in an extensive numerical example including the Coriolis term. At last, we like to point the reader's attention to the segmentation of the energy spectrum in Fig. 6.9. While the inertial range shows a power-law spectrum, the dissipative range shows an exponential decay. This result fits excellently into the phenomenological theory of turbulence by Kraichnan [16], and differs from the linear Galerkin method. In the latter case the energy spectrum does not show a distinct segmentation into an inertial and dissipative range (see for more illustrations [7, 10]). A challenge for the future is to extend the algorithm to the full set of equations noted in (2.6)-(2.9) in the compressible case.

REFERENCES

[1] F. BAER, G. PLATZMAN: *A Procedure for Numerical Integration of the Spectral Vorticity Equation.* J. Met., Vol. 18, pp. 393, 1961.

[2] W. BOURKE: *An Efficient, One-Level, Primitive-Equation Spectral Model.* Mon. Weather Rev., Vol. 100, pp. 683-689, 1972.

[3] J. P. BOYD: *Chebyshev and Fourier Spectral Methods.* 2nd Ed. (Revised), Dover Publications, Inc., Mineola, New York, 2001.

[4] M. E. BRACHET, M. MENEGUZZI, H. POLITANO, P. L. SULEM: *The Dynamics of Freely Decaying Two-Dimensional Turbulence.* J. Fluid Mech., Vol. 194, pp. 333-349, 1988.

[5] D. M. BRINK, G. R. SATCHLER: *Angular Momentum.* Oxford Library of the Physical Sciences, 1968.

[6] G. C. COREY, J. W. TROMP: *Fast Pseudospectral Algorithm in Curvilinear Coordinates.* C. Cerjan (ed.). Numerical Grid Methods and Their Application to Schrödinger's Equation, pp. 1-23, Kluwer Academic Publishers, Netherlands, 1993.

[7] A. DEBUSSCHE, T. DUBOIS, R. TEMAM: *The Nonlinear Galerkin Method: A Multiscale Method Applied to the Simulation of Homogeneous Turbulent Flows.* Theoret. Comput. Fluid Dynamics, Vol. 7, pp. 279-315, 1995.

[8] A. R. EDMONDS: *Drehimpulse in der Quantenmechanik.* Bibliographisches Institut, Mannheim, 1964.

[9] H. W. Elsaesser: *Evaluation of Spectral versus Grid Methods of Hemispheric Numerical Weather Prediction.* J. App. Meteorol., Vol. 5, pp. 246, 1966.

[10] M. J. Fengler: *Vector Spherical Harmonic and Vector Wavelet Based Non-Linear Galerkin Schemes for Solving the Incompressible Navier-Stokes Equation on the Sphere* PhD-thesis (submitted), University of Kaiserslautern, Department of Mathematics, Geomathematics Group, 2005.

[11] W. Freeden, T. Gervens, M. Schreiner: *Constructive Approximation on the Sphere (With Applications to Geomathematics).* Oxford Science Publications, Clarendon, Oxford, 1998.

[12] B. J. Hoskins, A. J. Simmons: *A Multi-Layer Spectral Model and the Semi-Implicit Method.* Quart. J. R. Met. Soc., Vol. 101, pp. 637-655, 1975.

[13] A. A. Il'in: *The Navier-Stokes and Euler Equations on Two-dimensional Closed Manifolds.* Math. USSR Sbornik, Vol. 69, No.2 , pp. 559-579, 1991.

[14] A. A. Il'in, A. N. Filatov: *On Unique Solvability of the Navier-Stokes Equations on the Two-dimensional Sphere.* Soviet Math. Dokl., Vol. 38, No. 1, pp. 9-13, 1989.

[15] R. W. James: *New Tensor Spherical Harmonics, for Application to the Partial Differential Equations of Mathematical Physics.* Phil. Trans. R. Soc. Lon. A 281, pp. 195-221, 1976.

[16] R. H. Kraichnan: *Inertial Ranges in Two-Dimensional Turbulence.* Phys. Fluids, Vol. 10, pp. 1417-1423, 1967.

[17] M. Marion, R. Temam: *Nonlinear Galerkin Methods.* Siam J. Numer. Anal., Vol. 26, No. 5, pp. 1139-1157, 1989.

[18] J. Norbury, I. Roulstone: *Large-Scale Atmosphere-Ocean Dynamics I/II. Analytic Methods and Numerical Models.* Cambridge, University Press, 2002.

[19] S. A. Orszag: *Transform Method for the Calculation of Vector-Coupled Sums: Application to the Spectral Form of the Vorticity Equation.* J. Atmos. Sci., Vol. 27, pp. 890-895, 1970.

[20] S. A. Orszag: *Turbulence and Transition: A Progress Report.* Proc. 5th Internat. Conf. on Numerical Methods in Fluids Dynamics, Lecure Notes in Physics, Vol. 59, pp. 32-51, 1977.

[21] A. Persson: *User Guide to ECMWF Forecast Products.* Technical Report, European Center for Medium-Range Forecast, 2000.

[22] J. Shen, R. Temam: *Nonlinear Galerkin Method Using Legendre Polynomials.* Proceedings of the International Conference on Nonlinear Evolution Partial Differential Equations, Beijing, China, 1993.

[23] R. Temam: *Navier-Stokes Equations. Theory and Numerical Analyis.* North-Holland, Amsterdam, New York, Oxford, 1979.

[24] C. Temperton: *On Scalar and Vector Transform Methods for Global Spectral Models.* Mon. Weather Rev., Vol. 119, pp. 1303-1307, 1991.
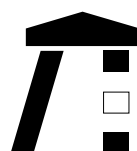
TECHNISCHE UNIVERSITÄT KAISERSLAUTERN

Informationen:

Prof. Dr. W. Freeden

Prof. Dr. E. Schock

Fachbereich Mathematik

Technische Universität Kaiserslautern

Postfach 3049

D-67653 Kaiserslautern

E-Mail: freeden@mathematik.uni-kl.de

schock@mathematik.uni-kl.de